UCRL-JC-131748
PREPRINT

Confined Combustion of TNT Explosion Products in Air

**A. L. Kuhl, J. Forbes, J. Chandler,
A. K. Oppenheim, R. Spektor,
R. E. Ferguson**

This paper was prepared for submittal to the
8th International Colloquium on Dust Explosions
Schaumburg, IL
September 21-25, 1998

August 31, 1998

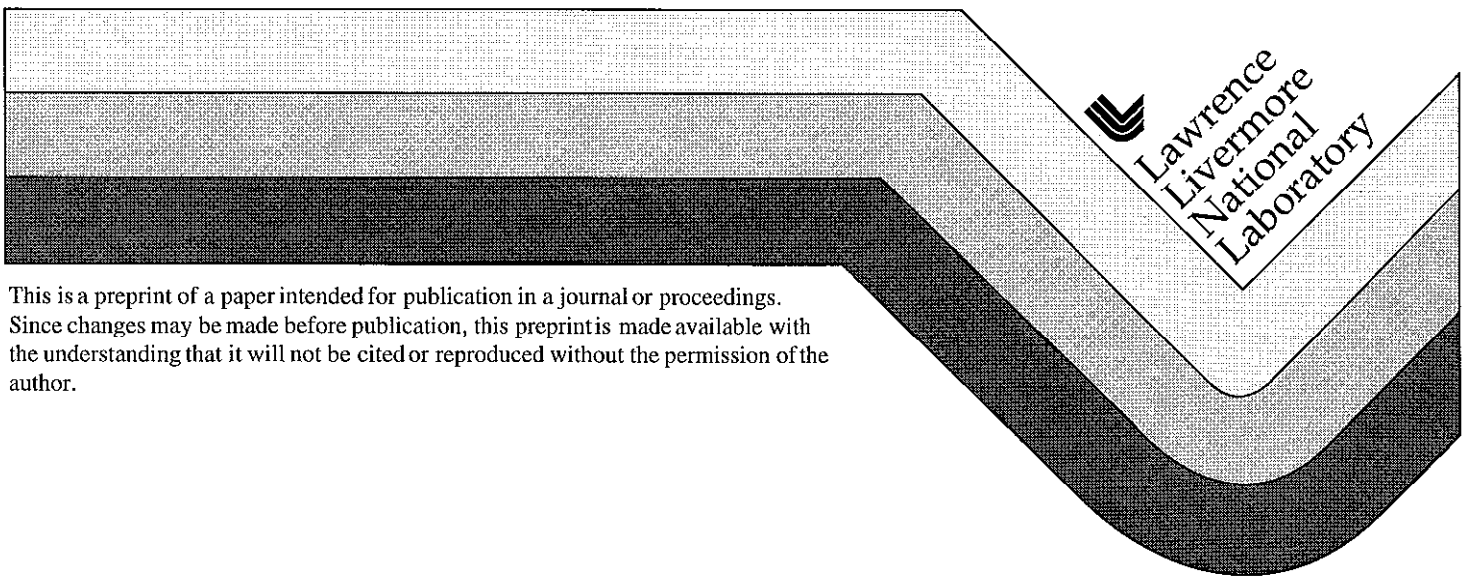

CONFINED COMBUSTION OF TNT EXPLOSION PRODUCTS IN AIR

A. L. Kuhl, J. Forbes & J. Chandler
Lawrence Livermore National Laboratory
Livermore, California, USA 94550

A. K. Oppenheim & R. Spektor
University of California
Berkeley, California, USA 94720

R. E. Ferguson
Krispin Technologies Inc.
Rockville, Maryland, USA 20850

Abstract

Effects of turbulent combustion induced by explosion of a 0.8 kg cylindrical charge of TNT in a 17 m^3 chamber filled with air, are investigated. The detonation wave in the charge transforms the solid explosive ($C_7H_5N_3O_6$) to gaseous products, rich (~20% each) in carbon dust and carbon monoxide. The detonation pressure (~210 kb) thereby engendered causes the products to expand rapidly, driving a blast wave into the surrounding air. The interface between the products and air, being essentially unstable as a consequence of strong acceleration to which it is subjected within the blast wave, evolves into a turbulent mixing layer—a process enhanced by shock reflections from the walls. Under such circumstances rapid combustion takes place where the expanded detonation products play the role of fuel. Its dynamic effect is manifested by the experimental measurement of ~3 bar pressure increase in the chamber, in contrast to ~1bar attained by a corresponding TNT explosion in nitrogen. The experiments were modeled as a turbulent combustion in an unmixed system at infinite Reynolds, Peclet and Damköhler numbers. The CFD solution was obtained by a high-order Godunov scheme using an AMR (Adaptive Mesh Refinement) to trace the turbulent mixing on the computational grid in as much detail as possible. The evolution of the mass fraction of fuel consumed by combustion thus determined exhibited the properties of an exponential decay following a sharp initiation. The results reveal all the dynamic features of the exothermic process of combustion controlled by fluid mechanic transport in a highly turbulent field, in contrast to those elucidated by the conventional reaction-diffusion model.

Introduction

The development of high explosives [1] started with the discovery of guncotton (nitrocellulose) by Schönbein [2] in 1846, and the discovery of Nitroglycerine ($C_3H_5N_3O_9$) by Sobrero [3] in 1847. During the next decade, Emmanuel Nobel, following Zinin and Trapp from St Petersburg, developed an industrial manufacturing process for Nitroglycerine (NG). In 1864, his son, Alfred Nobel, discovered that NG can be absorbed on Kieselguhr (a porous inert powder) thereby creating dynamite: a mixture of 75% NG and 25% Kieselguhr (also known then as Guhr dynamite, or Nobel's safety powder). In 1865, Alfred Nobel invented a detonator based on mercury fulminate—thereby providing strong ignition source needed for high explosives. In 1869, Nobel patented active dynamite, and in 1875, he patented gelatin dynamite. In 1869, Abel [4] discovered detonation waves in condensed explosives. In 1880, Nobel and Able [5] published their research on explosives. In 1881-2 Berthelot [6] with Vieille [7] were the first to measure the detonation velocity in gases. In 1881-3, Mallard and Le Chatelier [8] were the first to photograph deflagration-to-detonation transition (DDT) in gases by means of a drum camera. This was followed by Hugoniot's study [9] on detonation propagation in 1887-9, Munroe's investigation [10] on wave effects in guncotton in 1888, Chapman's paper [11] on explosions in gases in 1899, Dixon's measurements [12] of detonation velocities in 1893 & 1903, and Jouguet's publication [13] on mechanics of explosives in 1905-6. TNT was first used as an explosive in 1904 (although it had been used previously in the dye industry); its relative, Tritonal (80% TNT and 20% aluminum powder), is now used extensively in military applications. For a more-detailed chronology of early research on detonations, see Manson et al [14,15].

Monographs on condensed explosives date back to 1917, and include those of Marshall [16], J. Taylor [17], Bowden & Yoffe [18], Cook [19], W. Taylor [20], Belyaev [21], Johansson & Persson [22], Fickett & Davis [23], Mader [24], and Cheret [25]. Fundamental contributions to detonation theory were made by von Neumann [26], Zel'dovich & Kompaneets [27], Grushka & Wecken [28], Nettleton [29], and Perrson et al. [30]. Scientific investigations of TNT explosives were precipitated by the Second World War, such as the work of Goranson [31], with prominent contributions by Cybulski [32] who in 1943-1946 used a rotating-mirror camera to measure the detonation velocity in TNT, and others [33]-[38].

In contrast to condensed explosives, combustion is the oldest technology of mankind [39], and its literature is more extensive, as exemplified by the classical books of Jost [40], Lewis & von Elbe [41], Williams [42], Markstein [43], and the Princeton Series tractate *Combustion Processes* [44], as well as monographs originating from the Institute of Chemical Physics founded by Semenov [45,46], with prominent contributions by Zel'dovich [47]-[49], Frank-Kamenetskii [50], Kondrat'ev [51], Sokolik [52], and Shchelkin & Troshin [53], to mention just a few.

Investigated here are the macroscopic consequences of turbulent combustion in confined TNT explosions in air — in effect, a combination of the above two disciplines. The detonation wave in the charge transforms the solid explosive ($C_7H_5N_3O_6$) into gaseous detonation products, rich (~20% each) in carbon dust and carbon monoxide. Ornellas [54] performed experiments in a spherical stainless steel calorimeter with a volume of V = 5.28 liter. When 25-g TNT charges were detonated in a vacuum, the following composition of the expanded and cooled* products was measured by mass spectrometry:

$$C_7H_5N_3O_6 \Rightarrow 1.32N_2 + 1.6H_2O + 1.25CO_2 + 1.98CO + 3.65C_{(s)} + 0.46H_2 + 0.16NH_3 \equiv \mathfrak{F}$$

Also, an explosion energy of 1093 Cal/g was measured by calorimetric methods—in agreement with thermodynamic equilibrium calculations of the *"Heat of Detonation"* for TNT (based on the CHEETAH code [55]).

As is evident from the above relation, products of the explosion can serve as a fuel, $\mathfrak{F}$, which will react when mixed with oxygen, thereby forming combustion products $\mathfrak{CP}$. In other experiments [54], 25-g TNT charges were detonated in an oxygen atmosphere (pressurized to 2.46 bars), where the following composition was measured by mass spectrometry:

$$\mathfrak{F} + 5.3O_2 \Rightarrow 1.54N_2 + 2.65H_2O + 6.82CO_2 + 0.38CO \equiv \mathfrak{CP}$$

An explosion energy of 3575 Cal/g was measured by calorimetric methods—in agreement with thermodynamic equilibrium calculations of the *"Heat of Combustion"* for TNT (based on the CHEETAH code [55]). Thus, the explosion-induced mixing of the

* **Note:** once the products have cooled below 1800 K, the composition may be considered to be frozen.

TNT products with oxygen deposited an additional 2482 Cal/g of exothermic energy as a consequence of the turbulent combustion process. In the popular literature, this is known as "after-burning" in TNT explosions (see Dewey [56]). What was here-to-for unknown was the temporal evolution of that energy.

More recently, Wolanski [57] has conducted experiments in a calorimeter with a volume of *V=3.1* liters. 25-, 50- and 100-g TNT charges were detonated in argon and in oxygen-enriched air atmospheres. He measured a *"Heat of Detonation"* of 960 Cal/g in argon, and *a "Heat of Combustion"* of 3608 Cal/g in enriched air—in good agreement with Ornellas' measurements. He also measured the composition of the explosion products and pressure histories on the side wall. He used a combustion chamber (*V=38.5* liters) located in a 30-cm diameter Schlieren beam, to visualize the combustion process. His results will be reported at this Symposium.

Described here are the dynamics that exothermic process, namely turbulent combustion of TNT explosion products with air in a chamber—based on experiments, thermodynamic analysis and numerical simulations. Experiments (Section 2) were conducted in the 17-m^3 tank at the *High-Explosives Application Facility* (*HEAF*) of LLNL, where 0.8-kg cylindrical TNT charges were detonated in air and nitrogen atmospheres; pressure measurements were the main diagnostic. Oppenheim [58,59] has developed a methodolgy based on the inverse problem of combustion, to deduce the thermodynamic and thermochemical aspects of combustion in an enclosure. This model was used to analyze the experiments (Section 3), and thereby infer the mass-fraction burned from the pressure records. Based on the ideas Zel'dovich expressed *in The Mathematical Theory of Combustion and Explosions* (vid. especially Chapter 6) [49] as well as Shchelkin & Troshin's concepts in *Gasdynamics of Combustion* [53], Kuhl and Oppenheim have proposed a gasdynamic model [60] of un-mixed turbulent combustion at asymptotically-infinite Reynolds, Peclet and Damköhler numbers. This model, which was used previously to simulate the dynamics of an exothermic jet [61], was applied here to simulate exothermic dynamics in the *HEAF* experiments. The results reveal the dynamic features of exothermic process of combustion controlled by fluid-mechanic transport in a highly-turbulent field, in contrast to those elucidated by the conventional reaction-diffusion model. Numerical solutions are shown to be in satisfactory agreement with experimental results.

We note that the theme of this Symposium—*dust explosions*—may be considered as a problem of combustion in un-mixed (dust-air) systems induced by shocks waves

(explosions) in tunnels (confinement). The fundamental work of the Polish scientist Waclaw Cybulski, who made so many measurements of deflagrations and detonations [62] in dust-air mixtures in the experimental mine "Barbara", as reported in his monograph *Coal Dust Explosions and Their Suppression* [63], makes this extremely clear. It is in this context that the present work on confined combustion in explosions seems quite relevant to the theme of this Symposium.

Experiments

The experiments were conducted in an explosion chamber (Fig. 1), which can accommodate solid-explosive charges with a mass of 1.2 kg. The chamber was constructed as a cylindrical stainless steel tank (inner diameter D = 2.38 m and length L = 4 m) with a volume of V = 16.64 m^3. A pneumatically-actuated door mechanism allowed easy access for test setup. The charge was hung in the middle of the chamber (Fig. 2). For tests with a nitrogen atmosphere, the chamber was pumped down to a few torr, and filled with N_2 gas; this process was repeated several times until nitrogen concentrations greater than 99% were achieved.

The charge assembly is shown in Fig.3. It consisted of an 800-g TNT charge, a 50-g LX-10 booster, and a 25-g SE-1 detonator, with a total mass of 875 g. The TNT was pressed to a density of 1.63 g/cm^3, in the form of cylindrical plugs (5 cm in diameter and 9.1 cm long); three such plugs were then glued together with Eastman-910 adhesive, to form the final 800-g TNT charge (diameter d = 5 cm and length l = 27.34 cm).

The primary diagnostic consisted of five quartz pressure transducers (PCB Piezotronics Inc, Model 102A), mounted in a fixtures on the side wall of the test chamber (see Fig. 2), at approximately 130 cm distance from the charge. Signals were transmitted through coaxial cables and recorded on Tektronics oscilloscopes (TDS-540) at a sampling rate of 500 MHz. Sensor elements were thermally shielded with black plastic tape. Also, beaded thermal couples (Omega model CHAL-022) were used to estimate the temperature of the post-explosion products gases. After the test, the chamber gases were sampled, and analyzed with a VG mass spectrometer (30-01) to determine the chemical composition of the combustion products.

Experiments in an air atmosphere were used to investigate the macroscopic (pressure) effects of confined combustion of TNT with air, while experiments in a nitrogen atmosphere were used to evaluate the confined-explosion effects of detonating

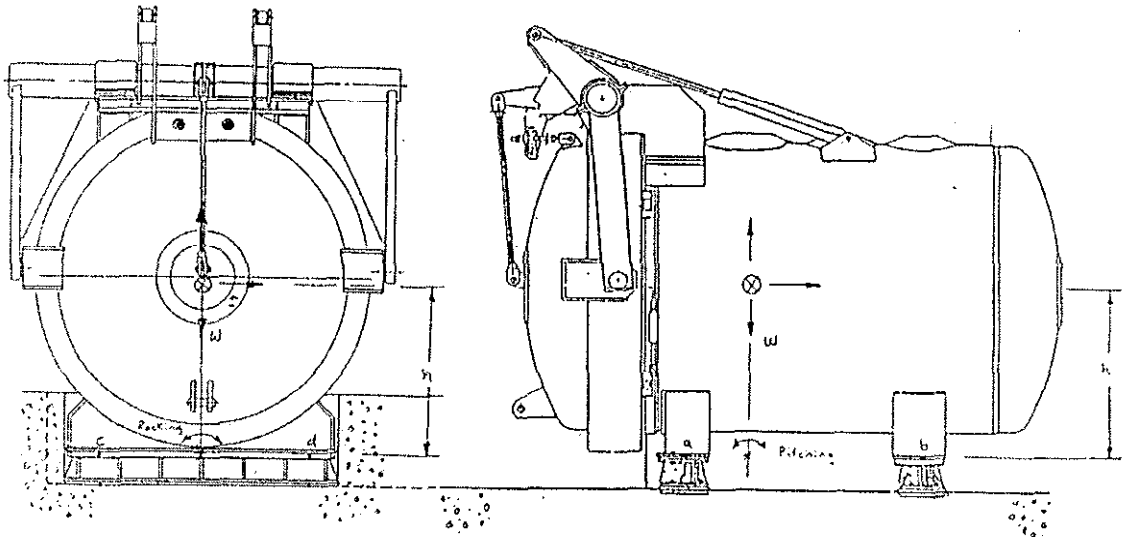

Figure 1. Schematic of the 16.6-m^3 explosion/combustion chamber used for 1-kg TNT tests.

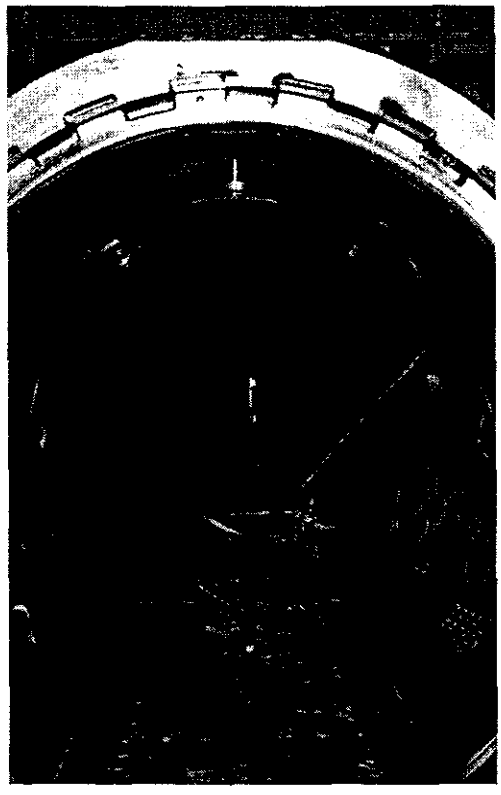

Figure 2. Photograph of the chamber interior, showing the test setup.

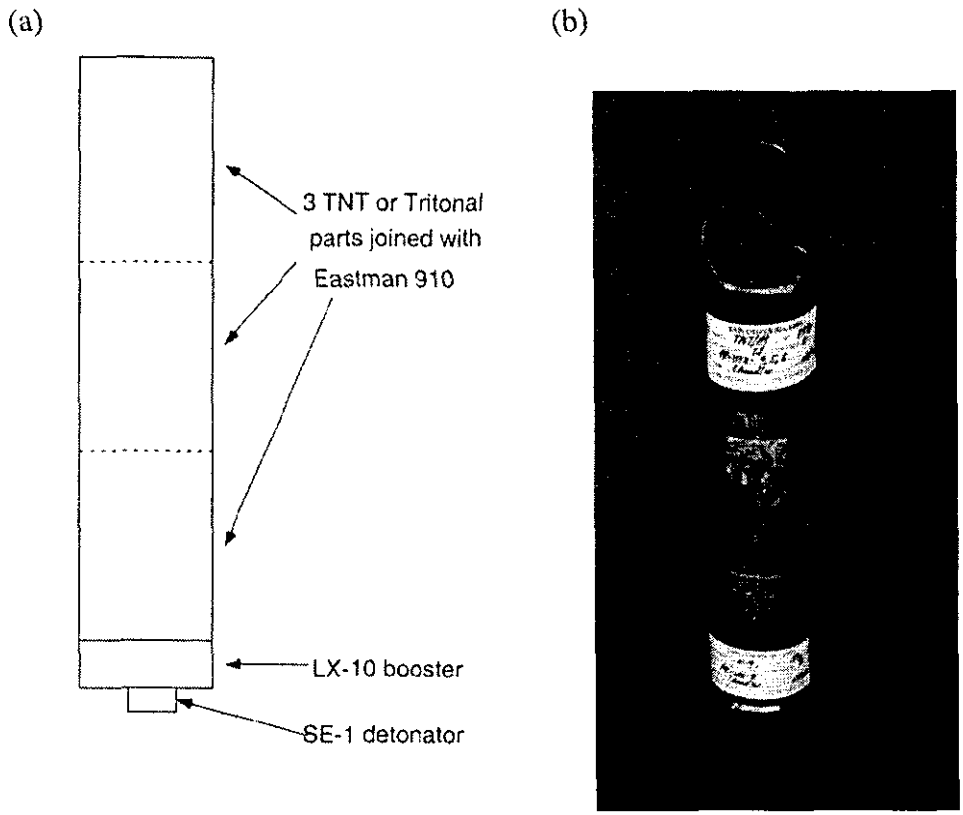

Figure 3. Configuration of the 800 g cylindrical TNT charge: (a) schematic; (b) photograph.

the TNT charge. These tests were repeated with Tritonal charges (a military explosive consisting of 80% TNT with 20% aluminum powder)—to evaluate the potential enhancement due to aluminum combustion. The mass of the Tritonal charge (770 g) was selected to give the same energy as the TNT charge, based on equilibrium calculations with the CHEETAH code [55].

The ignition sequence was as follows: first, SE-1 detonator was fired with a 10 kilo-volt pulse; this caused the LX-10 booster to fire, which transmitted a detonation wave into the main charge. Thus, the cylindrical charge was "end detonated"—thereby depositing approximately 956 k-Cal in the products gases.

Expansion of these products created a three-dimensional blast wave—whose pressure signature was recorded by gauges on the chamber wall. A typical example of such pressure records is shown in Fig.4. Compared there are the results of a confined TNT explosion in an air (test #4) and nitrogen (test #1). Initially the blast waves are very similar; but after about 2 ms, the pressure record in the air case becomes much larger due to combustion effects.

A suite of pressure records for a TNT charge explosion and combustion in air is presented in Fig. 5 (test #3); a similar set for a Tritonal charge is depicted in Fig. 6 (test #1). The major peaks are due to shock reverberations within the chamber, while the minor oscillations are due to turbulence.

In order to extract a "mean" pressure from these signals, the records were time-averaged with a sliding window of 7.5 ms (corresponding to the longitudinal acoustic period of the tank). Figure 7 clearly demonstrates the effects of combustion: late-time mean pressures for a TNT explosion in air are about 2.8 bars, while mean pressures for TNT explosion in nitrogen are about 0.85 bars Their ratio (2.8 bars)/(0.85 bars)=3.3 is in good agreement with the ratio: (heat of combustion)/(heat of detonation)=(3575 Cal/g)/(1093 Cal/g)= 3.27 as reported by Ornellas [54]. Similar combustion effects were found in the Tritonal tests (Fig. 8). Thus, one can conclude that the enhanced pressure found for tests in air atmospheres is due to the exothermic energy deposition by turbulent combustion.

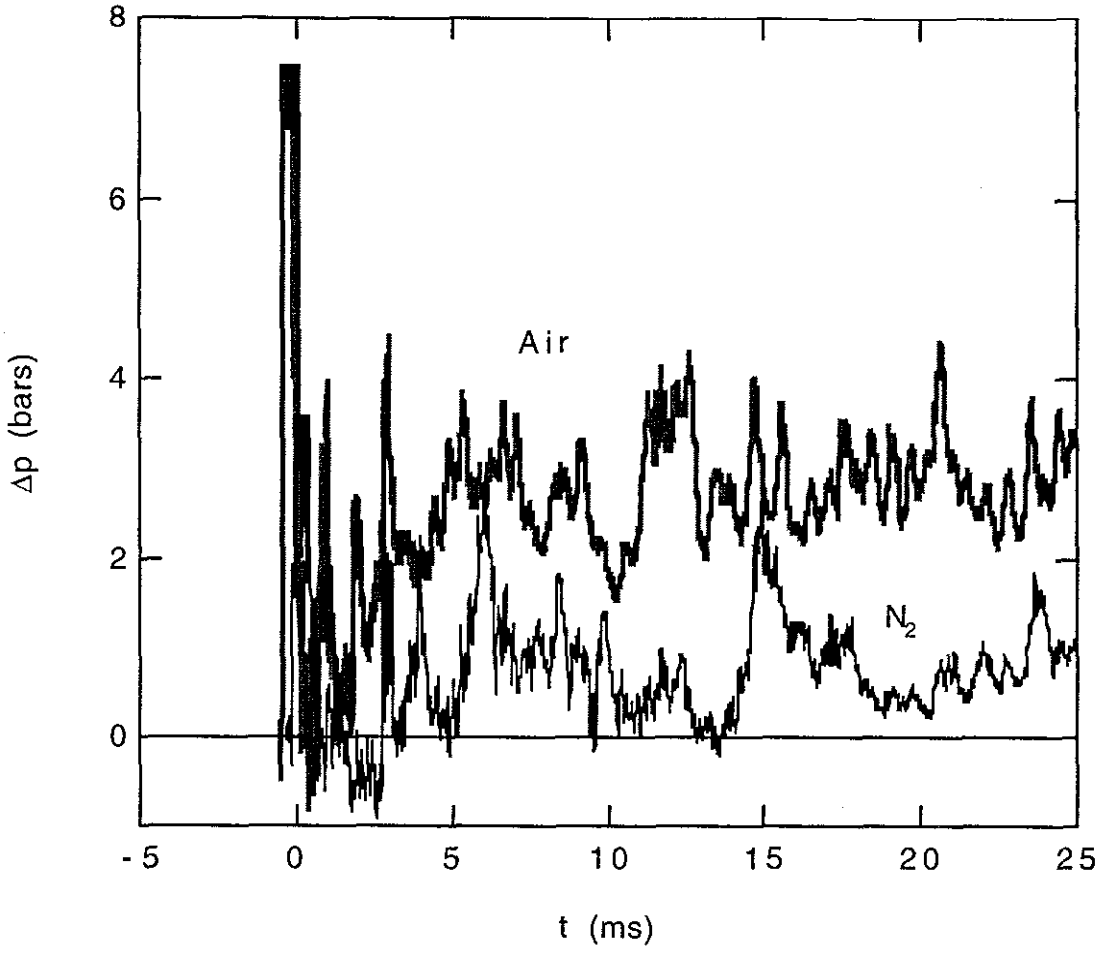

Figure 4. Over-pressure history measured for a TNT explosion in an air atmosphere (test #4, gauge 2) and in a nitrogen atmosphere (test #1, gauge 1).

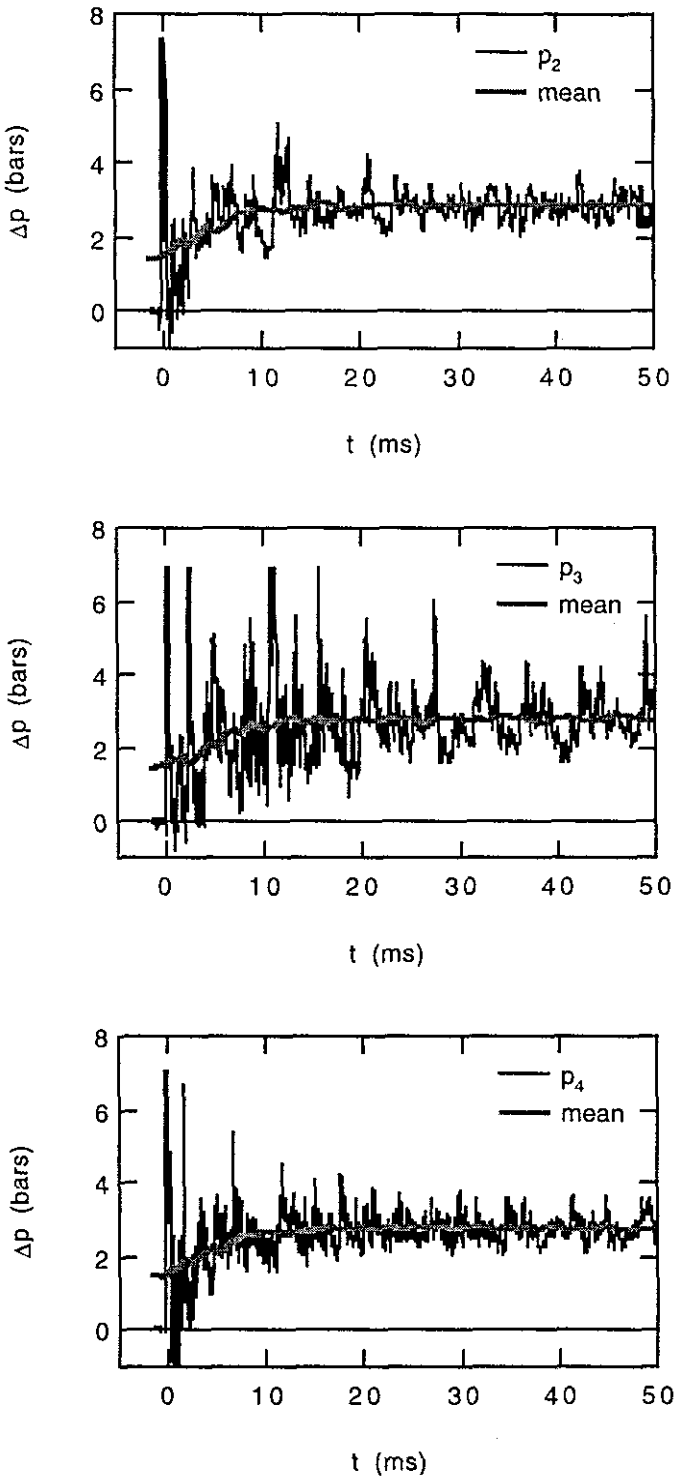

Figure 5. Over-pressure histories measured in a TNT explosion/combustion in an air atmosphere (test #3).

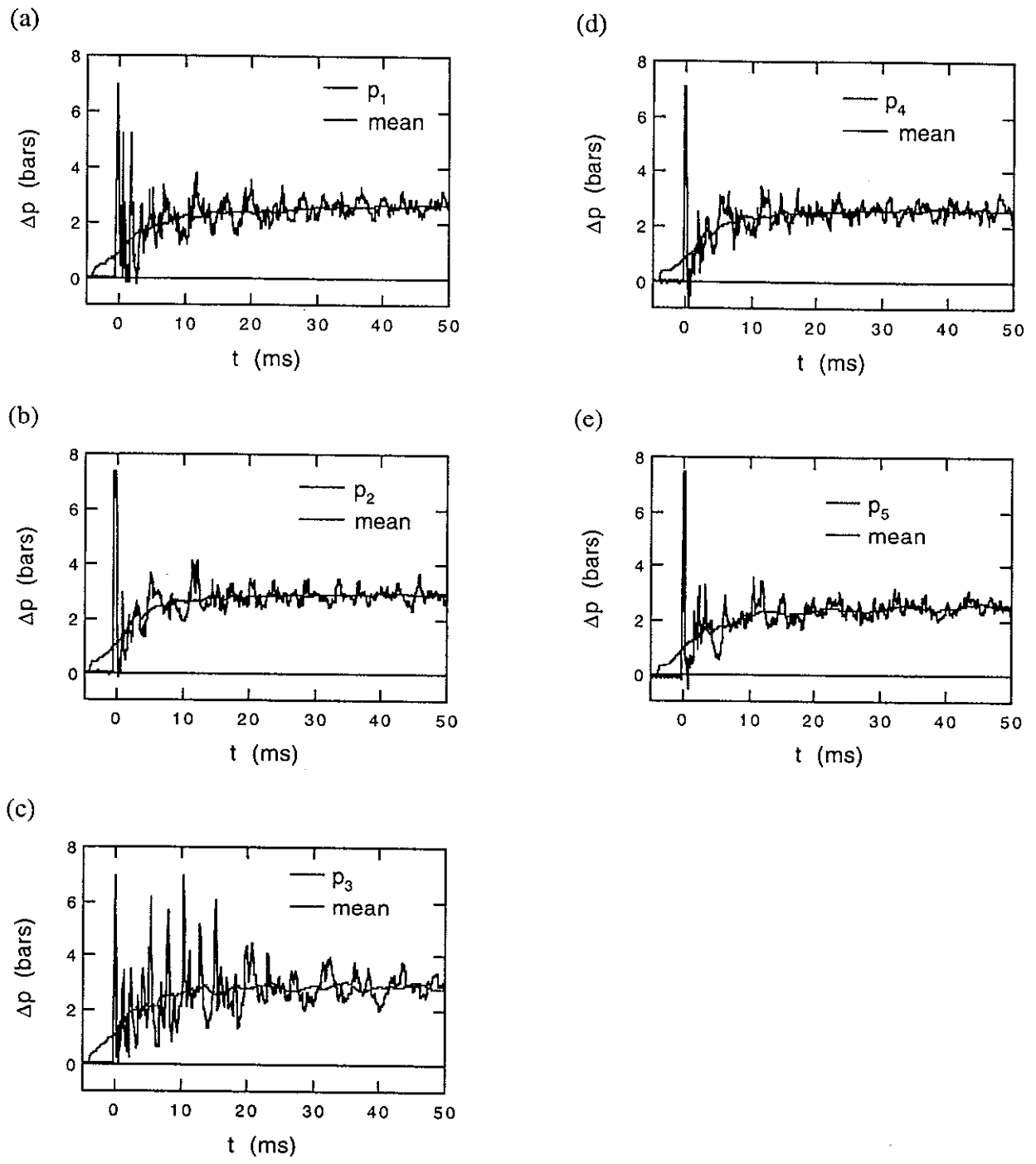

Figure 6. Over-pressure histories measured in a Tritonal explosion/combustion in an air atmosphere (test #1).

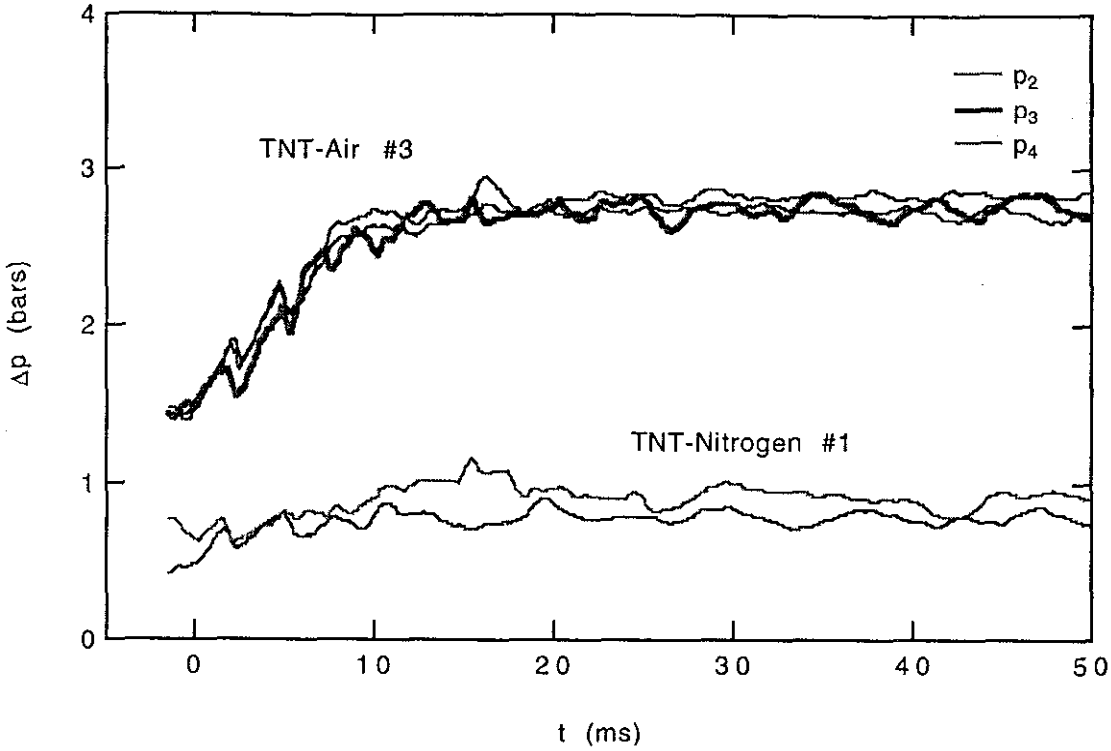

Figure 7. Comparison of mean (time-averaged) pressure histories for turbulent combustion of TNT explosion products in air (test #3) versus turbulent mixing of TNT products in nitrogen (test #1).

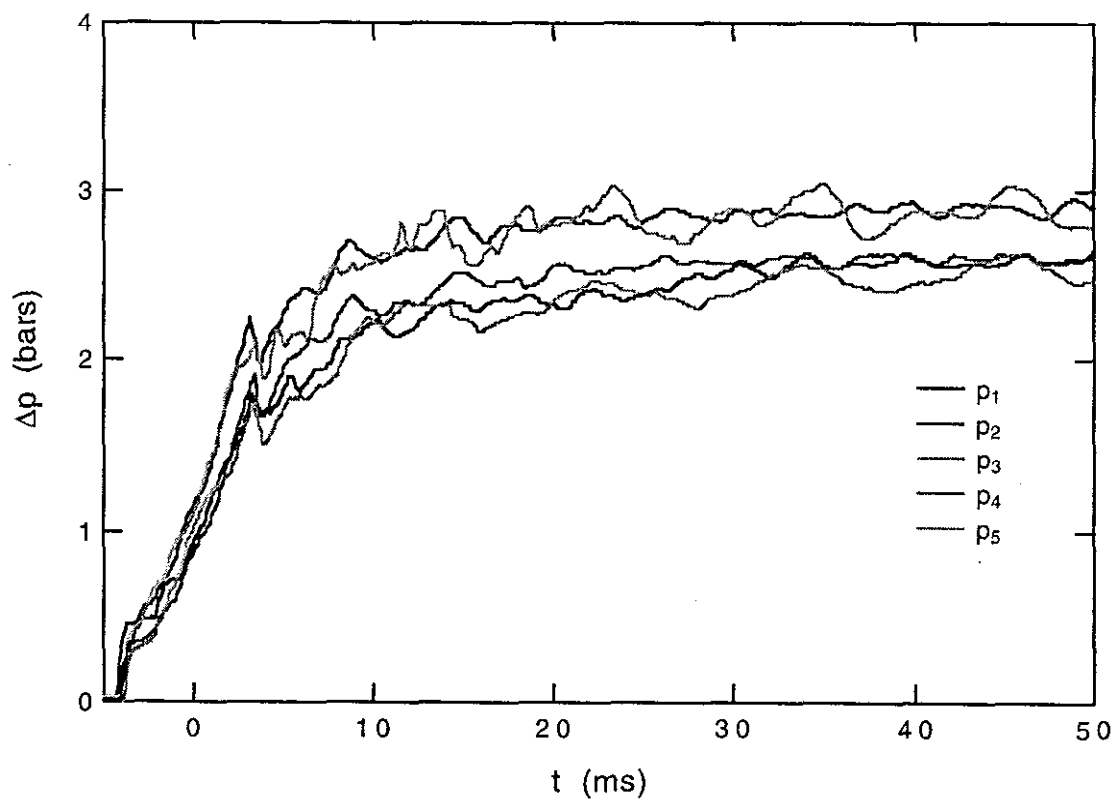

Figure 8. Mean (time-averaged) pressure histories for turbulent combustion of Tritonal explosion products in air (test #1).

Thermodynamic Analysis

Inverse Problem

The prime purpose of the experimental program reported here is to explore the mechanism of post-explosion combustion, or 'after-burn,' in a vessel of fixed volume. Posed thus is an inverse problem: reveal the dynamics with which fuel is consumed by the exothermic process of combustion from its dynamic yield: the measured pressure profile. The latter is, as a rule, full of noise as a consequence of the reverberating shock fronts of the original blast wave. The solution, reported here, involved, therefore, three tasks: *(i)* extract the signal from the noise recorded by the pressure sensor; *(ii)* determine the thermodynamic properties of the working substance; *(iii)* deduce, by thermodynamic analysis, fuel consumption as a function of time.

Properties

In order to bring up the intrinsically dynamic nature of the combustion system, instead of temperature, as is usually done, adopted here as the principal thermodynamic reference parameter is

$$\mathbf{w}_K = \mathbf{p}_K \mathbf{v}_K \tag{1}$$

where $\mathbf{p}$ and $\mathbf{v}$ denote the thermodynamic pressure and specific volume, while $K = \Phi, \Omega, R, P$ and S, referring, respectively, to fuel, oxidizer, reactants, products and system. For the sake of clarity, the variables are expressed here (in this section) by bold block letters, while the constants are in normal block type.

The thermodynamic pressure, $\mathbf{p}$, (i.e. the thermodynamic parameter of state, rather than the aerodynamic variable in the equation of motion) is considered as spatially uniform. Hence, the effect of pressure gradients is disregarded, so that

$$\mathbf{p}_\Phi = \mathbf{p}_\Omega = \mathbf{p}_R = \mathbf{p}_P = \mathbf{p}_S = \mathbf{p}(\mathbf{t}) \tag{2}$$

where $\mathbf{t}$ denotes time—the primary independent variable of the problem. In view of this, pressure can be considered as a measure of time, whereby all the thermodynamic variables are solely functions of pressure. The inverse problem under study is thus in the domain of ordinary differential equations.

The thermodynamic properties of the components are expressed most conveniently in terms of a *Le Chatelier diagram* (vid. Oppenheim & Maxson, [58], [59])—a plot of the loci of their states on the plane of internal energy, **u**, as a function of **w**, specified by (1). Salient features of this diagram are illustrated in Fig. 9.

Loci of states of the components are marked by their symbols, Φ, Ω, and P for, respectively, the fuel, oxidizer and products, while i and f denote their initial and final states. The line denoted by R delineates the locus of states of the substance to be consumed by combustion—referred to here as the reactants. It is made out of Φ and Ω, mixed in proportions at which they react. Thus, at any pressure, in terms of $\varpi \equiv \mathbf{u}, \mathbf{w}$,

$$\varpi_R = F_r \varpi_\Phi + (1 - F_r)\varpi_\Omega \tag{3}$$

where $F_r = 1/(1+\lambda_r\sigma)$, with λ_r denoting the local excess-oxidizer coefficient (primarily air), while σ is the stoichiometric oxidizer/ fuel ratio. Unless the reactants are premixed, $\lambda_r = 1$. Since R is not an *a priori* component, it is expressed by a broken line. The products of this mixture are considered to be at thermodynamic equilibrium.

Slopes of the loci of states, within the scope of their applicability to a representative problem of a closed combustion system, are expressed by C_K $(K = \Phi, \Omega, R, P)$. If a component behaves as a perfect gas, $C_K \equiv c_{vK}/R = 1/(\gamma_K - 1)$ — a relation that applies to the products.

A change of state taking place in the course of the exothermic process of corresponds to a jump from a point on *curve R* to one on *curve P*. Points *hp* and *uv* on *P*, represent the states of equilibrium attained, respectively, at the initial enthalpy and pressure and at the initial internal energy and volume—thus marking the *initial* and *final* states of the products established in the ideal case of an *isentropic* and *isochoric* process. Denoted by *HR (LHV)* and *AHR* are the popularly employed parameters of 'Heat Release" (or the 'Lower Heating Value') and 'Apparent Heat Release'. The results of an analysis based on this concept, associated, as is usually done, with the perfect gas assumption, are presented by points i and f on the straight line at a slope of c_V/R. In contrast to them, the corresponding initial and final points, representing the results of our analysis, are located on *curve P* below *uv* an *hp*—as a consequence as the loss of internal energy due to heat transfer to the walls of the enclosure.

Noting that, as evident in Fig. 9, the loci of states of component fluids are, within the regimes of their applicability, practically linear, they are expressed by straight lines,

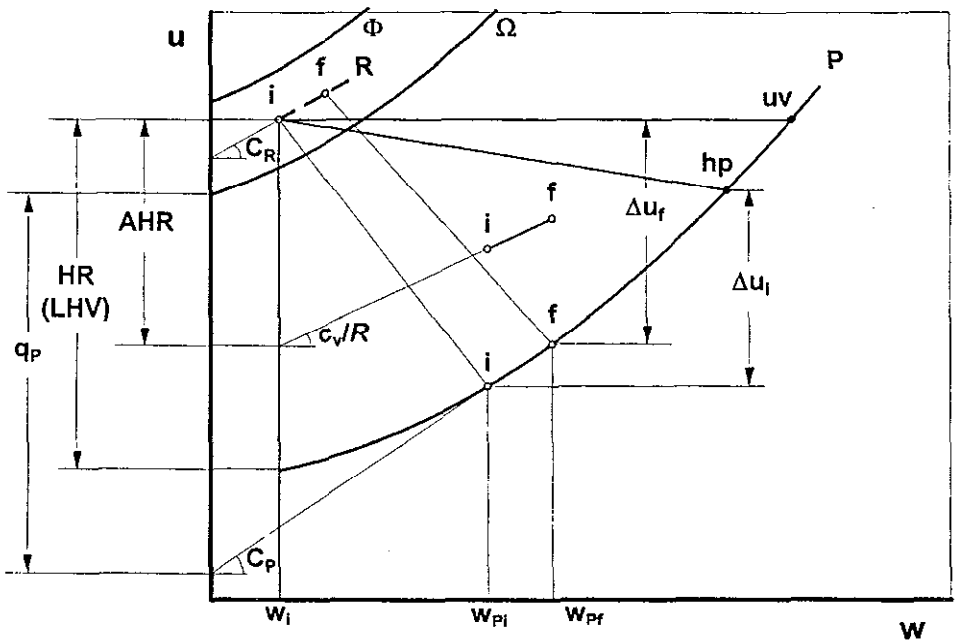

Figure 9. Salient features of the *Le Chatelier diagram.*

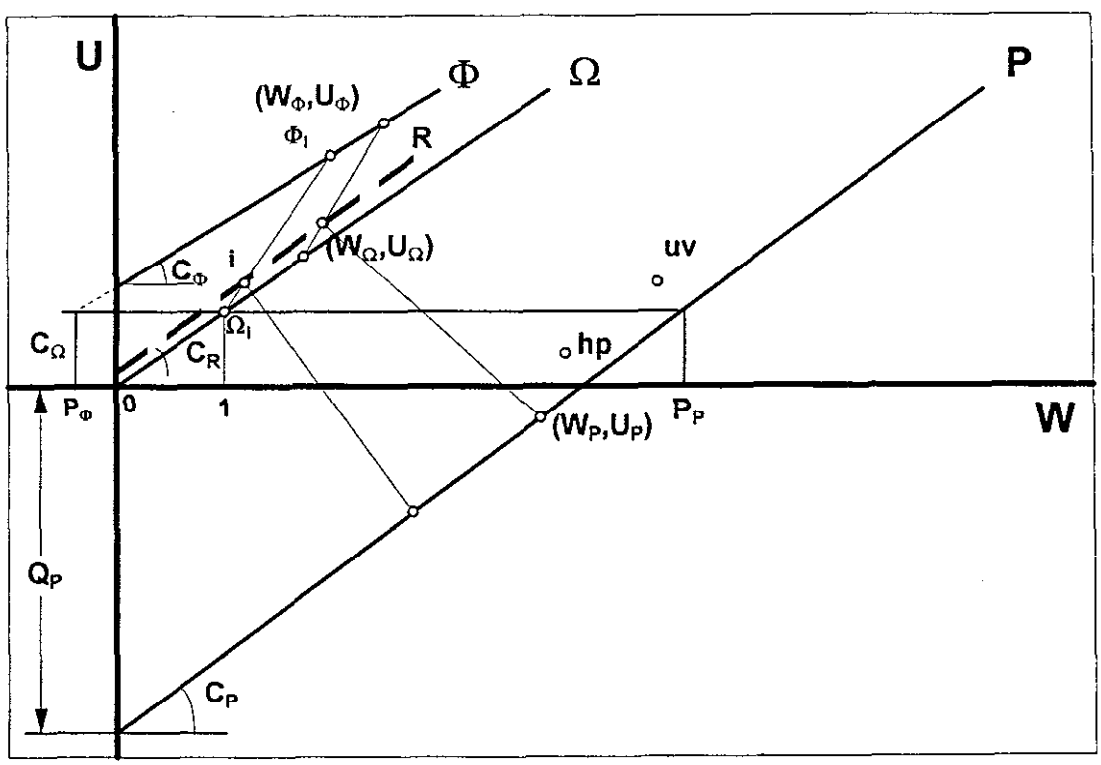

Figure 10. Linearized version of the *Le Chatelier diagram.*

as shown on Fig 10. Of particular significance here is the pivotal role, played by the fiducial point at $\mathbf{w} = 0$ and $\mathbf{u} = u_O$, located at the intersection of the straight line representing the locus of states of the oxidizer, Ω, with the axis of ordinates.

The two components of the thermodynamic reference parameter, pressure and specific volume are then normalized with respect to their values at the initial state, i, to be expressed in terms of $\mathbf{P} \equiv \mathbf{p}/p_i$ and $\nu \equiv \mathbf{v}/v_i$, while, with $K = R, P$,

$$\mathbf{W}_K \equiv \frac{\mathbf{w}_K}{w_{\Omega i}} \tag{4}$$

$$\mathbf{U}_K \equiv \frac{\mathbf{u}_K - u_o}{w_{\Omega i}} = C_K \mathbf{W}_K - Q_K \tag{5}$$

where, by virtue of the way the fiducial point is defined, $Q_\Omega \equiv 0$, while, for $(K = \Phi, P)$, one has $Q_K \equiv q_K / w_{\Omega i}$. The latter can be expressed in terms of $P_K \equiv (Q_K + C_\Omega)/C_K$. Concomitantly, the energy loss in a vessel of fixed volume

$$\mathbf{U}_e \equiv \frac{\mathbf{q}}{w_{\Omega i}} = \mathbf{\Omega} \tag{6}$$

where $\mathbf{q}$ is the energy lost by heat transfer to the walls.

Balances

With the thermodynamic properties of the reacting system thus expressed, the analysis is based on three conservation principles: the balance of mass, the balance of volume and the balance of energy.

The **mass balance** is depicted on Fig. 11, where $\mathbf{Y}_K$ represents mass fractions of components. The mass fraction of products is adopted as a progress parameter and plays, therefore, the role of the abscissa axis; it is written as $\mathbf{Y}$ devoid of a subscript. The initial state is marked by subscript *i*. Thus, at $\mathbf{Y} = 0$, the mass-fraction of fuel in the charge to be consumed by combustion is $Y_{\Phi i} \equiv F_i = 1/(1 + \lambda_i \sigma)$, where λ_i is the *initial* excess-oxidizer coefficient of the system. The final state is denoted by *f*. Then $Y_{\Phi f} = 0$, whereas the final mass-fraction of products is

$$Y_f = \frac{F_i}{F_r} \tag{7}$$

Then, as evident from Fig. 11,

$$\mathbf{Y}_\Phi = F_i - F_r \mathbf{Y} \tag{8}$$

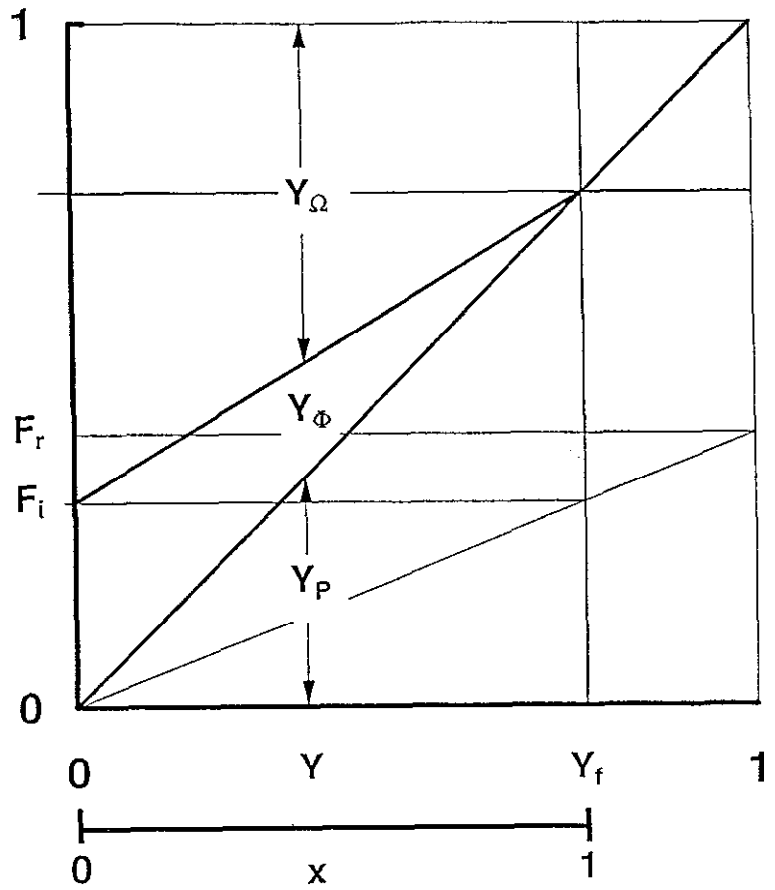

Figure 11. Diagram of mass balance.

while the rest is

$$\mathbf{Y}_{\Omega} = 1 - \mathrm{F}_i - (1 - \mathrm{F}_r)\mathbf{Y} \tag{9}$$

A primary objective of the thermodynamic analysis is the evaluation of the effectiveness with which fuel is utilized in the course of the exothermic process of combustion. Its mass fraction consumed thereby (fraction of fuel burned) is thus

$$\mathbf{x} \equiv \frac{\mathbf{Y}}{\mathrm{Y}_f} = \frac{\mathrm{F}_r}{\mathrm{F}_i}\mathbf{Y} \tag{10}$$

presented by the lower-scale abscissa in Fig.11.

The **volume balance** is, in view of (1) and (2), specified by

$$\mathbf{Y}_{\Phi}\mathbf{W}_{\Phi} + \mathbf{Y}_{\Omega}\mathbf{W}_{\Omega} + \mathbf{Y}_{P}\mathbf{W}_{P} = \mathbf{W}_{S} \tag{11}$$

Using (8) and (9), one finds

$$\mathbf{W}_{P} = \mathbf{W}_{R} + \frac{\mathbf{W}_{S} - \mathbf{W}_{\Omega} - \mathrm{F}_i(\mathbf{W}_{\Phi} - \mathbf{W}_{\Omega})}{\mathbf{Y}} \tag{12}$$

where $\mathbf{W}_{R} \equiv \mathrm{F}_r\,\mathbf{W}_{\Phi} + (1 - \mathrm{F}_r)\mathbf{W}_{\Omega}$, according to (3).

The energy balance is expressed in terms of internal energies, so that, in terms of their normalized form of (3), (4) and (5),

$$\mathbf{Y}_{\Phi}\mathbf{U}_{\Phi} + \mathbf{Y}_{\Omega}\mathbf{U}_{\Omega} + \mathbf{Y}_{P}\mathbf{U}_{P} = \mathbf{U}_{S} = \mathrm{U}_{Si} - \mathbf{U}_{e} \tag{13}$$

wherefore

$$\mathrm{U}_{Si} = \mathrm{U}_{\Omega i} + \mathrm{F}_i(\mathrm{U}_{\Phi i} - \mathrm{U}_{\Omega i}) \tag{14}$$

Products

Utilizing (8), (9), and (12), the energy balance (13) can be solved for the products fraction

$$\mathbf{Y} = \frac{\underline{\Delta}_{S} - \underline{\Delta}_{\Omega} + \mathrm{F}_i[(\mathrm{W}_{\Phi i} - 1)\underline{\Delta}_{S} + \underline{\Delta}_{\Omega} + \underline{\Delta}_{\Phi}] + \kappa}{\Omega_{P} - (\mathrm{k}_{P} - 1) - \underline{\Delta}_{\Omega} + \mathrm{F}_r[\underline{\Delta}_{\Omega} + \underline{\Delta}_{\Phi} + \Lambda_{\Phi} + \Omega_{\Phi} + (\mathrm{k}_{\Phi} - 1)]} \tag{15}$$

where $\mathrm{k}_{K} \equiv \mathrm{C}_{K}/\mathrm{C}_{\Omega}$, $\Omega_{K} \equiv \mathrm{Q}_{K}/\mathrm{C}_{\Omega}$ and $\kappa \equiv \mathrm{Q}/\mathrm{C}_{\Omega}$; or, with $\mathrm{P}_{K} \equiv (\mathrm{Q}_{K} + 1)/\mathrm{k}_{K}$,

$$\mathbf{Y} = \frac{\underline{\Delta}_{S} - \underline{\Delta}_{\Omega} + \mathrm{F}_i[(\mathrm{W}_{\Phi i} - 1)\underline{\Delta}_{S} + \underline{\Delta}_{\Omega} + \underline{\Delta}_{\Phi}] + \kappa}{\mathrm{k}_{P}(\mathrm{P}_{P} - 1) - \underline{\Delta}_{\Omega} + \mathrm{F}_r[\underline{\Delta}_{\Omega} + \underline{\Delta}_{\Phi} + \Lambda_{\Phi} - \mathrm{k}_{\Phi}(\mathrm{P}_{\Phi} - 1)]} \tag{15'}$$

where $\underline{\Lambda}_S \equiv \underline{k}_P(\underline{W}_S - 1)$, $\underline{\Lambda}_\Omega \equiv (\underline{k}_P - 1)(\underline{W}_\Omega - 1)$, $\underline{\Lambda}_\Phi \equiv (k_\Phi - k_P)W_{\Phi i}(\underline{W}_\Phi - 1)$, and $\Lambda_\Phi \equiv (k_\Phi - k_P)(W_{\Phi i} - 1)$, whereas

$$W_{Si} = 1 + F_i(W_{\Phi i} - 1) \tag{16}$$

The normalized reference parameters for the reactants are expressed in terms of **P** by virtue of a polytropic relation

$$\underline{W}_K \equiv W_K / W_{Ki} = \mathbf{P}^{1-1/n_K} \tag{17}$$

wherefore, in terms of the isentropic efficiency

$$\eta_s \equiv \frac{h - h_{CJ}}{h_{is} - h_{CJ}} \tag{18}$$

with h denoting the enthalpy, and subscripts *CJ* and *s*, the Chapman-Jouguet state and its entropy, the polytropic index is

$$n_K = 1/[1 - (1 - \gamma_K^{-1})] \tag{19}$$

In view of (10), equations (15) provide expressions for the mass fraction of fuel consumed by the exothermic process of combustion, **x**, as an explicit function of **P**, except for heat transfer to the walls, κ. If, however, the exothermic system is adiabatic, κ = 0, then, as a consequence of (15), the mass fraction of products, **Y**, becomes entirely a function of **P**. Yielded thus, by virtue of (10), is the time profile of the mass fraction of fuel consumed by the exothermic process of combustion, **x**.

Fuel

In reducing pressure data for this purpose, special attention must be paid to the singular nature of the exothermic process at its bounds, corresponding to states *i* and *f*. The initial state, *i*, is, as pointed out here at the outset, 'the essential singularity of combustion.' It is marked then by a sharp corner between the axes of a saddle point. The final state, *f*, on the other hand, is located at a smooth maximum, characteristic of a nodal point.

In an enclosure of fixed volume, **P** is a monotonic function of time (during the exothermic process of combustion), and thus directly suitable then for use as a progress parameter. In its normalized form, it becomes

$$\Pi = \frac{\mathbf{P} - 1}{\mathrm{P}_f - 1} \tag{20}$$

To cater, especially, to the singularity at *i*, for the thermodynamic analysis, this parameter must be expressed in an analytic form – a task accomplished in the simplest manner by regression to a polynomial. Provided thereby is the identification of the parameters of the initial and final states. At the final outcome, Π can be related directly to the mass fraction of fuel consumed by the exothermic process, yielding a functional relationship $\mathbf{x}(\Pi)$ in the form of either a power law or a constrained exponential (vid. next section). In view of this, our thermodynamic analysis can be considered as serving no other purpose than the determination of such a functional relationship. Since, in the prevalent case of a power law, its reduction to a proportionality is so conceptually straightforward, this simplification became quite popular (rendering thus effectively all the considerations of the thermodynamic analysis presented here redundant—at a cost of a significant loss of information). Nevertheless, this approximation may serve, a useful purpose—as a preliminary estimate.

Dynamics

The consumption of fuel occurring in the course of the exothermic process of combustion exhibits all the features of a dynamic system. This is brought out as follows. As a consequence of the singular behavior at its bounds, the rate of fuel consumption – the parameter expressing *de facto* $\mathrm{d}\mathbf{M}_b/\mathrm{d}\mathbf{t} = \dot{\mathbf{x}}$, invoked here at the outset as the manifestation of exothermicity, must conform with the following conditions. In terms of $\Theta \equiv \mathbf{t} / \mathrm{T}$, where T is the life time,

@ $\Theta = 0$: $\dot{\mathrm{x}} = \dot{\mathrm{x}}_i > 0$—a property marking the start of the exothermic process,

@ $\Theta = 0$: $\dot{\mathrm{x}} = 0$—the salient feature of its end state.

A function satisfying these conditions is expressed by

$$\dot{\mathbf{x}} = (\dot{\mathrm{x}}_i + \mathbf{x})(1 - \Theta)^{\delta} \tag{21}$$

with $\delta > 0$. Its derivative is given by

$$\ddot{\mathbf{x}} = \frac{(1-\Theta)^{\delta+1} - \delta}{1 - \Theta}\dot{\mathbf{x}} \tag{22}$$

whence $\ddot{\mathbf{x}} = 0$ @ $\Theta^* = 1 - \delta^{1/(\delta-1)}$, thereby specifying the time coordinate of the inflection point.

The integral of (21) provides an expression for the fraction of fuel consumed by the exothermic process of combustion in the form of a normalized, constrained exponential involving two parameters, α and β,

$$\mathbf{x} = \frac{e^{A} - 1}{e^{\alpha} - 1} \qquad \text{with} \qquad \mathbf{A} \equiv \alpha[1 - (1 - \Theta)^{\beta}] \qquad (23)$$

The function $\mathbf{x}(\Theta)$ expressed above is exhibited by an S curve. If, however, the initial rate, $\dot{\mathbf{x}}_i$, is sharp enough—as it is in the case of strong ignition—the profile of $\mathbf{x}$ is devoid of inflection. The integral relation takes then the form

$$\mathbf{x} = (1 + \mathbf{x}_i)\frac{e^{B} - 1}{e^{\alpha} - 1} - \mathbf{x}_i \qquad \text{with} \qquad \mathbf{B} \equiv \alpha[1 - (\frac{1 - \Theta}{1 - \Theta_i})^{\beta}] \qquad (24)$$

where $\mathbf{x}_i = \frac{1 - e^{-\alpha}}{1 - e^{-\Gamma}}$, while $\Gamma \equiv \alpha/(1 - \Theta_i)^{\beta}$—a function involving three parameters, α, β and Θ_i.

The mass fraction of fuel consumed by the exothermic process of combustion acquires then the role of displacement, its rate (the rate of burn) plays the role of velocity, and variation of the rate – the role of acceleration. The results of the thermodynamic analysis are reduced thus to the plots of normalized, constrained exponential, whose parameters specify all the dynamic properties of the combustion system.

Résumé

The thermodynamic analysis presented here is based on four principles: (i) thermodynamic properties of the components; (ii) balance of mass; (iii) balance of volume; (iv) balance of energy. The first provides the functional relationship between the internal energies, $\mathbf{u}_K$, and the corresponding thermodynamic reference parameters, $\mathbf{w}_K \equiv \mathbf{p}_K \mathbf{v}_K$ ($K = \Phi, \Omega, R, P$)—thereby eliminating $\mathbf{u}_K$ from further relationships. The second permits the mass fractions of all the components to be expresses in terms of one of the $\mathbf{Y}_K$, namely $\mathbf{Y}$. The third furnishes an expression for $\mathbf{w}_P$ in terms of the reference parameters of the reactants and $\mathbf{Y}$. On this basis, the fourth yields $\mathbf{Y} = \mathbf{Y}(\mathbf{w}_\Phi, \mathbf{w}_\Omega)$ or $\mathbf{Y} = \mathbf{Y}(\mathbf{w}_R)$, and the expression used to eliminate $\mathbf{w}_P$ is then utilized to determine its value. The reference parameters of the reactant species are then expressed in terms of pressure. The coordinates of $\mathbf{w}_K$ ($K = \Phi, \Omega$) are finally expressed

in terms of pressure by means of polytropic relations. Thus, in the absence of energy loss by heat transfer to the walls, which turned out to be here the case (vid. next section), the mass fraction of fuel consumed by the exothermic process of combustion becomes solely a function of pressure. Upon this background, dynamic features of the exothermic process become expressible in terms of a normalized constrained exponential function, and all their properties are described concisely by three parameters of this function: α, β, Θ_i.

Thermodynamic parameters

For post-explosion combustion of TNT, pressure transducer records were obtained in two tests: one in a nitrogen atmosphere and then in air. The first set of data provides information on the chemical system forming the fuel for the second test. Both are presented on Fig. 12. As evident there, pressure data are full of 'noise,' caused by the reverberating shock fronts stemming from the original explosion. The 'signal' is then retrieved by regression.

The base line, obtained by first order polynomial regression, and the profile of the pressure generated by the exothermic process of combustion, obtained by fourth order polynomial regression, are provided in Fig. 13. The sharp intersection between them identifies the coordinates of the initial state, *i*, while the point of vanishing derivative fixes the final state, *f*. Their values are displayed on the graph. It appears then that, according to the analytic expression for the pressure profile, the life time of the exothermic process of combustion is T = 1.3399 + 17.5828 = 18. 9227 msec, while P_f = 3.82339 / 1.7429 = 2.1940, so that $\mathbf{P} = 1 + 1.1940\Pi$, or $\mathbf{p} = (1.7428 + 2.0810\Pi)$ bars.

The thermodynamic properties of fuel (i.e., the products created by the detonation of the TNT charge) are then determined by evaluating of the change of state they undergo in expanding isentropically from the Chapman-Jouguet state to the initial pressure, p_i. This has been accomplished by the use of *CHEETAH* [55] and *STANJAN* [73]. The results are depicted on the enthalpy – entropy plane in Fig. 14 and on the enthalpy – temperature plane of Fig. 15. Shown on both of them are lines of constant reference pressures of 2 and 4 bars, representing the initial and final states of the exothermic process. Displayed there are also are states of constant isentropic efficiency, η_S, specified by (18). The thermodynamic parameters of fuel at the initial and final state are provided in Table 1, where C refers to *CHEETAH* and S to *STANJAN.* There is practically no difference between the specific volumes computed by the two codes, while

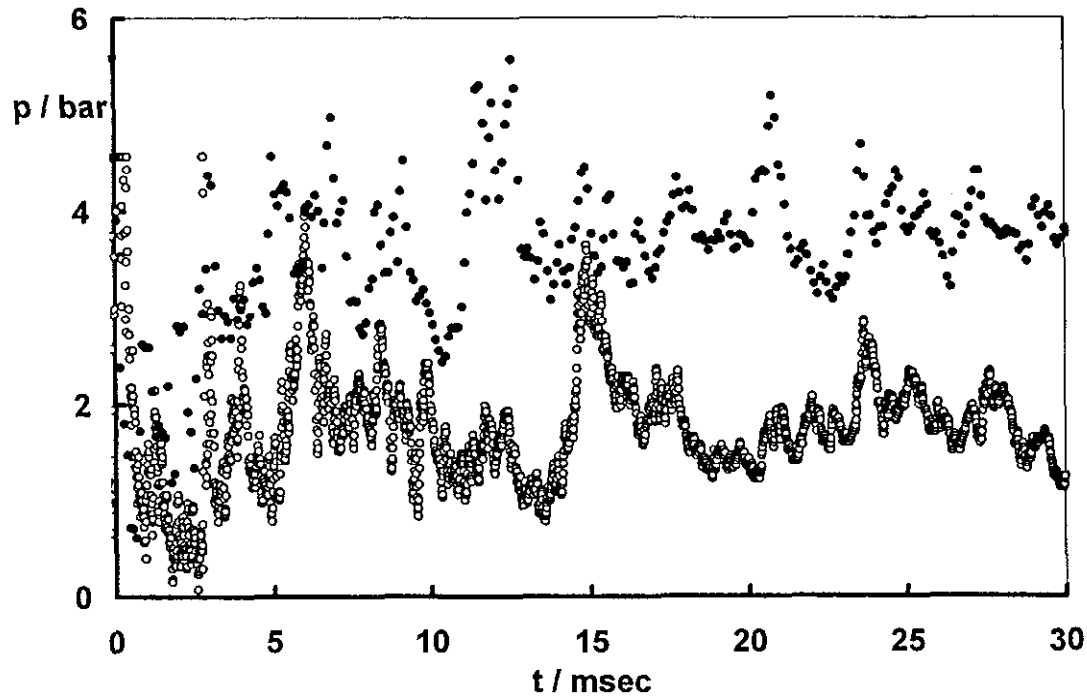

Figure 12. Pressure records.

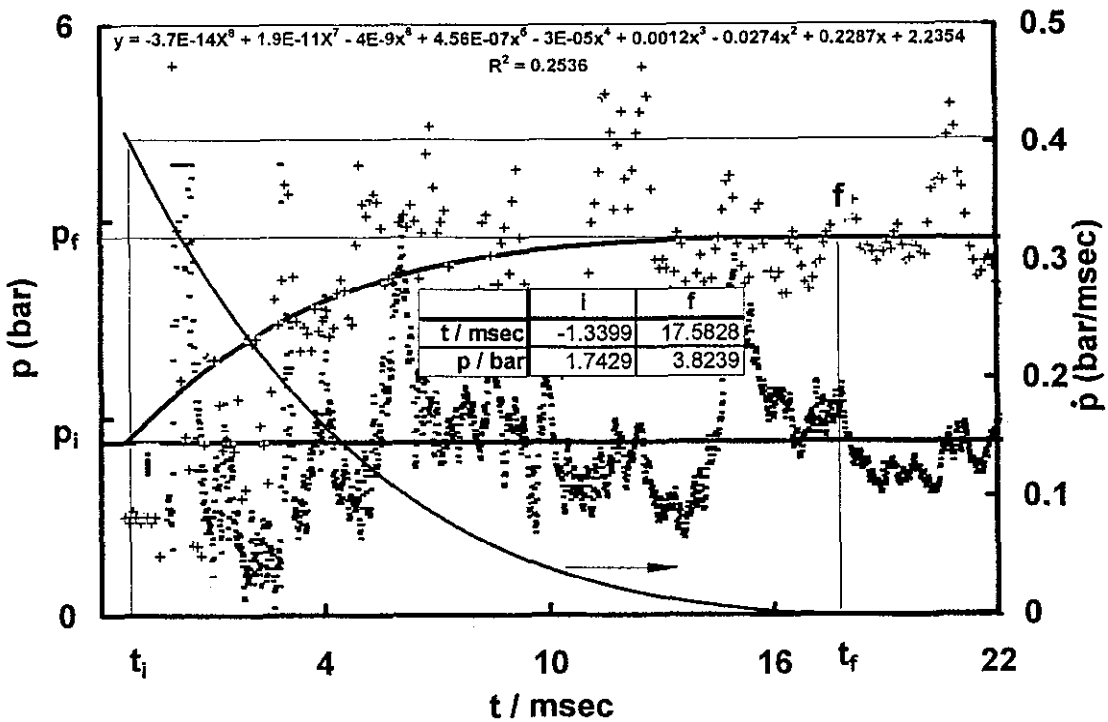

Figure 13. Analytic expression for pressure profile.

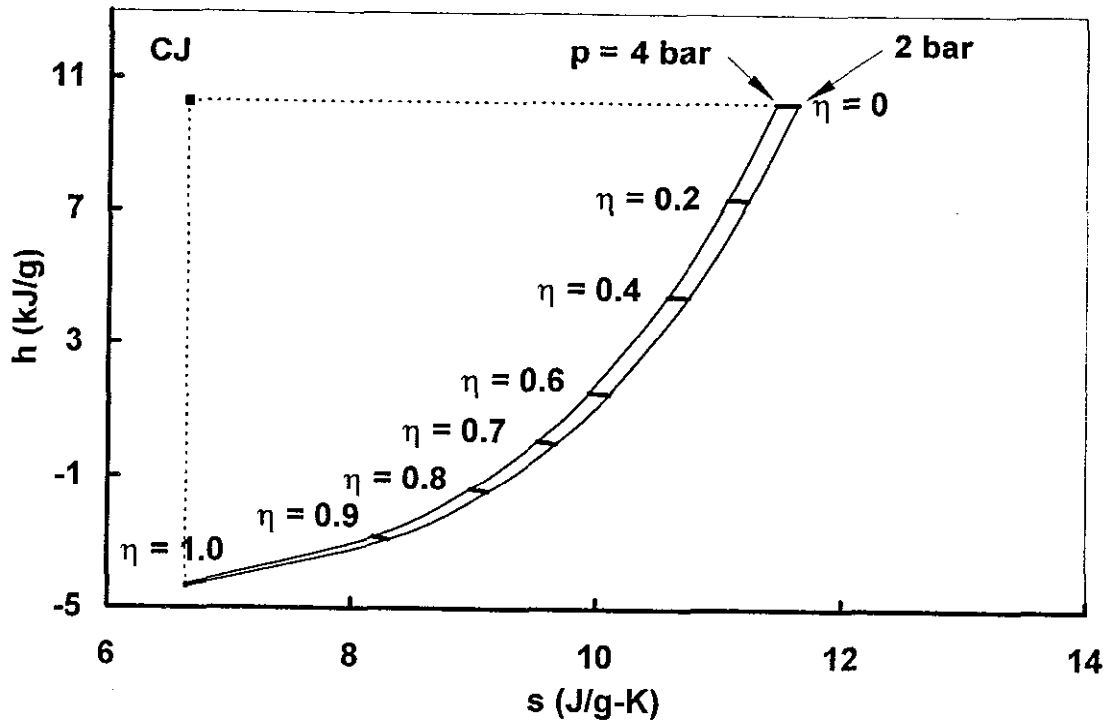

Figure 14. Enthalpy-entropy diagram of expansion from the Chapman-Jouguet state at a set of isentropic efficiencies.

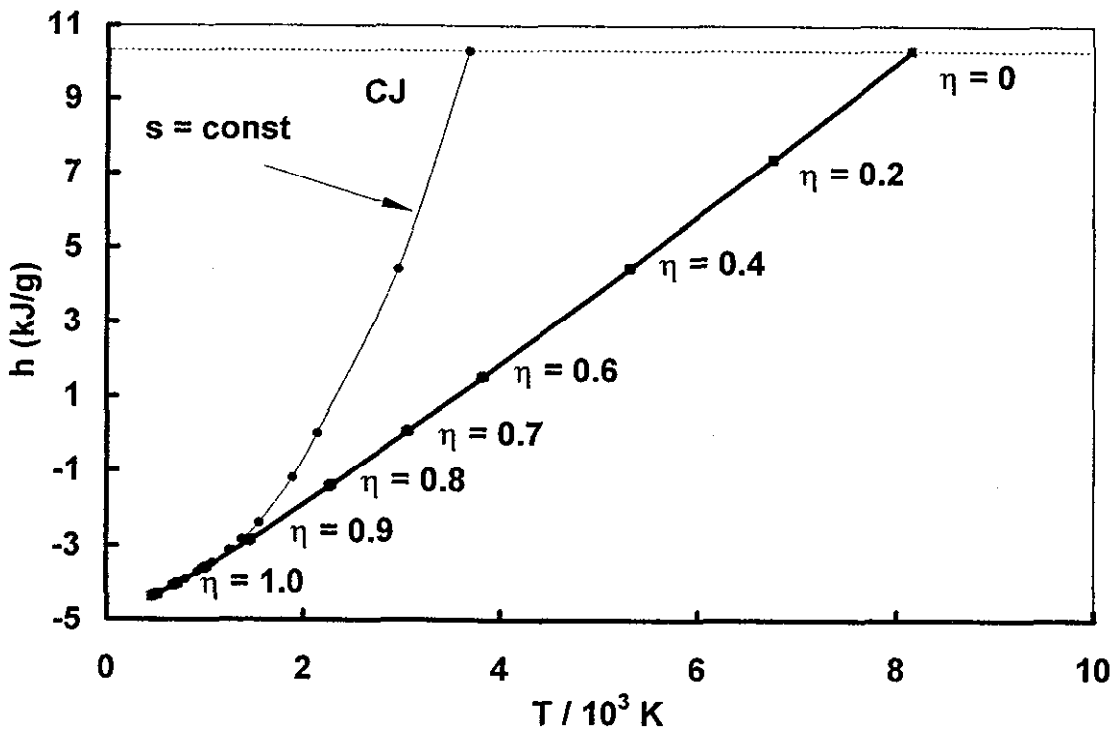

Figure 15. Enthalpy-temperature diagram of expansion from the Chapman-Jouguet state at a set of isentropic efficiencies.

internal energies differ by a constant (the reference energy). Thus, in changing from *CHEETAH* to *STANJAN*, it is sufficient to take into account only the latter, as specified in the last column on the first row. Moreover it is apparent from Fig. 15, that a fairly large departure from the isentrope corresponds to a relatively small change of the isentropic efficiency, so that, the simplification of taking $\eta_S = 1$, i.e., according to (19), $n_R = \gamma_R$, is well justified.

Table 1. Thermodynamic Properties of fuel at initial and final states

η	State	p	T	v cc/g			w kJ/g			u kJ/g		
		bar	K	C	S	Δ (%)	C	S	Δ (%)	C	S	Δ
1	i	2	457	565	563	0.31	0.114	0.114	0.31	-4.49	-4.82	0.33
	f	4	524	325	323	0.52	0.132	0.131	0.52	-4.42	-4.75	0.33
0.8	i	2	2262	2793	2790	0.11	0.566	0.565	0.11	-2.01	-2.35	0.34
	f	4	2300	1420	1418	0.16	0.575	0.575	0.16	-1.95	-2.29	0.34
0.7	i	2	3050	3766	3762	0.10	0.763	0.762	0.10	-0.74	-1.10	0.36
	f	4	3082	1903	1900	0.13	0.771	0.770	0.13	-0.68	-1.04	0.36
0.6	i	2	3816	4710	4706	0.09	0.954	0.953	0.09	0.54	0.16	0.38
	f	4	3842	2372	2369	0.11	0.961	0.960	0.11	0.58	0.20	0.38

Chemical composition

Composition of the mixture constituting the post-explosion fuel was determined from mass spectroscopic measurement of "post-shot" products of TNT explosion in nitrogen. The data were incomplete, in that they did not include the concentrations of C, H_2O and N_2. The missing information is provided here by analysis based on atom balances.

Considered here, in particular, is Run No. 17029 (reported on 3/12/96), for which the charge was made out of 875 gm of TNT and 19.11 kg of N_2. The latter was determined for an enclosure 16.6 m^3 in volume, with nitrogen at 1 bar and 300K. The results of the spectroscopic analysis are shown in Table 2. Mole fractions, X_i^0, of measured species are displayed in the first column. Listed in the second column are the

stoichiometric coefficients, ν_i, of a postulated chemical transformation expressed by the chemical balance

$$C_7H_5N_3O_6 + \nu_n N_2 = \nu_1 CO_2 + \nu_2 CO + \nu_3 CH + \nu_4 H + \nu_5 O_2 + \nu_6 N_2 + \nu_7 C + \nu_8 N_2 \qquad (25)$$

or, in terms of the measured mole fractions,

$$\begin{aligned} &C_7H_5N_3O_6 + \nu_n N_2 = \\ &\quad = \alpha[X_1^0\, CO_2 + X_2^0\, CO + X_3^0\, CH_4 + X_4^0\, H_2 + X_5^0\, O_2] + \nu_6 N_2 + \nu_7 X_7\, C + \nu_8 N_2 \end{aligned} \qquad (26)$$

while $$\nu_n = \frac{19.11 \times 10^3 \times 227}{875 \times 28} = 177$$

Table 2. Mole fractions and stoichiometric coefficients

i	Species	Experiment			Theory	Δ (%)*
		X_{oi}	ν_i	X_i	ν_i	
	$C_7H_5N_3O_6$		1	0.006		
n	N_2		177	0.994		
1	CO_2	0.72	1.29	0.68	0.99	23.06
2	CO	0.84	1.50	0.80	2.01	-34.1
3	CH_4	0.05	0.09	0.05	0.16	-74.8
4	H_2	0.26	0.46	0.25	0.16	65.69
5	O_2	0.02	0.04	0.02	0.00	100
6	N_2		178.50*	95.02	1.50	99.16
7	C		4.12	2.20	3.84	6.985
8	H_20		1.86	0.99	2.01	-8.03

* ν_6 = 1.50 in vacuum

** $\Delta = (\nu_{ie}-\nu_i)/\nu_{ie}$

Table 3. Atomic Population

i	Species	C	N	O
1	CO_2	1	0	2
2	CO	1	0	1
3	CH_4	1	0	0
4	H_2	0	0	0
5	O_2	0	0	2
6	N_2	0	2	0
7	C	1	0	0
8	H_20	0	0	1

Atom balances, obtained by multiplying the transposed matrix of atomic population, displayed in Table 3, by the vector of the stoichiometric coefficients, listed on the right side of (26), are expressed by the following four equations

O: $$[2X_1^0 + X_2^0 + 2X_3^0]\alpha + \nu_8 = 6 \qquad (27)$$

H: $$[4X_3^0 + 2X_4^0]\alpha + 2\nu_8 = 5 \qquad (28)$$

C: $$[X_1^0 + X_2^0 + X_3^0]\alpha + \nu_7 = 7 \qquad (29)$$

N: $$2\nu_6 = 3 + 2\nu_n \qquad (30)$$

They yield $\alpha = 1.879$ with ν_6, ν_7 and ν_8 displayed in the second column of Table 2, together with $\nu_i = \alpha X_i^0$ for i = 1-5. Thereupon one obtains $X_i = \nu_i / \Sigma\nu_i$ listed there in the third column. Provided, for comparison, in the fourth and fifth columns, are the corresponding results obtained from thermodynamic calculations carried out by the use of *CHEETAH*, as described in Figs. 14 and 15. Data of Table 3 are rearranged to identify the components of the post-explosion combustion, the fuel, Φ, and the oxidizer, Ω, a substance consisting of inert components of the products of detonation and air, as displayed on Table 4, while the results corresponding to the fourth column in Table 3 are provided in the third and fourth columns. There is a significant departure from the data of Table 3, associated with the identification of $C_{(s)}$ and $C_{(g)}$ and the two top entries in the first and second column in Table 4. Its background is provided in the next section.

Table 4. Chemical composition

i	Comp.	Species	Experiment		Theory	
			ν_i	M_i (gm)	ν_i	M_i (gm)
1	Φ	C(s)	1.52	70.2	3.84	177.18
2		C(g)	2.60	120.1		
3		CO	1.50	161.7	2.01	216.89
4		CH_4	0.09	5.5	0.16	9.58
5		H_2	0.46	3.6	0.16	1.23
6	Ω	O_2	0.04	4.4	0.00	0.00
7		N_2	1.51	162.8	1.50	161.16
8		CO_2	1.29	217.7	0.99	167.49
9		H_20	1.86	128.6	2.01	138.95
10	Air:	O_2	139	4437.8		
11		N_2	522	14607.3		
12	Air:	O_2	5.28	650.5	5.23	644.34
13	stoichiometric	N_2	19.86	2141.2	19.67	2120.94

Table 5. Match

	C(g) = 0	C(g) > 0
F_i	0.018	0.018
F_r	0.115	0.115
Y_f	0.158	0.158
Y_{pfn}	2.037	2.064
Y_{pd}	8.015	13.0799
Y_{pf}	0.25411	0.158
x_{pf}	1.60542	0.997

Fuel consumption

Mass fractions, F_i, F_s [F_r for a stoichiometric mixture], $Y_f = F_i / F_s$, Y_{pfn} [numerator of (15) with $\kappa = 0$], Y_{fd} [denominator of (15)] and $Y_{pf} = Y_{pfn} / Y_{fd}$, evaluated on this basis, are presented in the first column in Table 5. Normally $Y_{pf} / Y_f =$

$x_{pf} < 0$, so that $\kappa > 0$. However here evidently the opposite turned out to be the case, as $x_{pf} > 0$, meaning that $\kappa < 0$ (!).

In an effort to rationalize this anomaly, we investigated many possibilities. Since the postulate that $\kappa < 0$ means that the exothermic process of combustion to be, in effect, endothermic [by, say, heat transfer from the walls], it was considered unlikely to occur. Thus, the only acceptable possibility was that the combustion system was adiabatic and, hence $\kappa = 0$, while $F_r = F_s$, the latter expressing a basic condition for the intrinsically unmixed post-explosion combustion system. This left two alternatives: either some of the carbon in the explosion products became unavailable for post-combustion, or part of the carbon, which was in a solid state at the Chapman-Jouguet condition, became partially sublimated in the course of expansion to the initial pressure, p_i. As it turned out from our calculations, the former could not satisfy the condition of $\kappa = 0$ and $F_r = F_s$. Hence the latter was finally accepted as the most plausible. Matching parameters satisfying these conditions were evaluated by iteration and are presented in the second column in Table 5. Concomitant stoichiometric coefficients of solid and gaseous carbon have been incorporated in Table 4.

It should be noted that the initial state of the exothermic process of combustion is thus not at equilibrium. The sublimation of carbon took place as a consequence of rapid expansion from the extremely high pressure and temperature of the Chapman-Jouguet state. The relaxation time to reach equilibrium at the initial state, when carbon is again in solid phase, was then longer than the induction time (ignition delay), so that combustion started before it could be established.

Upon this background, the thermodynamic properties of the fuel, Φ, and oxidizer, Ω, identified in Table 4, as well as of the reactants, R, and products, P, were evaluated by the use of *STANJAN*. The results are presented on the *Le Chatelier* diagram Fig. 16. Yielded thereby, by linear regressions to initial and final points, are their slopes, C_K, and intersects with the axis of $(w = 0, u_{K0})$, of which, by definition, $u_{\Omega 0} = 0$, whence $q_K = u_0 - u_{K0}$.

A summary of the thermodynamic parameters of the components ('equations-of-state') thus evaluated, is provided by Table 6. Their profiles with respect to pressure and time are presented in Figs. 17 and 18, respectively.

The dynamic properties of the system are displayed on Fig. 19 in terms of the normalized constrained exponential for pressure, **P**, and the mass fraction of fuel

consumed by the exothermic process of combustion, **x**. The two are practically identical as a consequence of the dominant role of the first term in the denominator of (15) and the absence of κ, so that, as evident on Fig. 17, **x**, varying here from 0 to 1, appears as a linear function of **P**. The results of our analysis, of relevance to the dynamic nature of the system, are thus expressed in terms of just three parameters: α, β and Θ_i, of the normalized constrained exponential function starting beyond the point of inflection, whose values are noted on the diagram.

Table 6. Equation-of-State parameters

K	Φ	Ω	R	P
C_K	2.56	2.71	2.69	5.12
k_K	0.94	1	0.99	1.89
P_K	-56.85	1	-4.44	4.75
Q_K	-148	0	-14.66	21.58
P_{RK}	-51.12	6.41	1	7.61
Q_{RK}	-133	14.66	0	36.24
γ_K	1.39	1.37	1.37	1.20

$w_{\Omega l} = 0.1281$ kJ/gm , $u_o = 1.4441$ kJ/gm

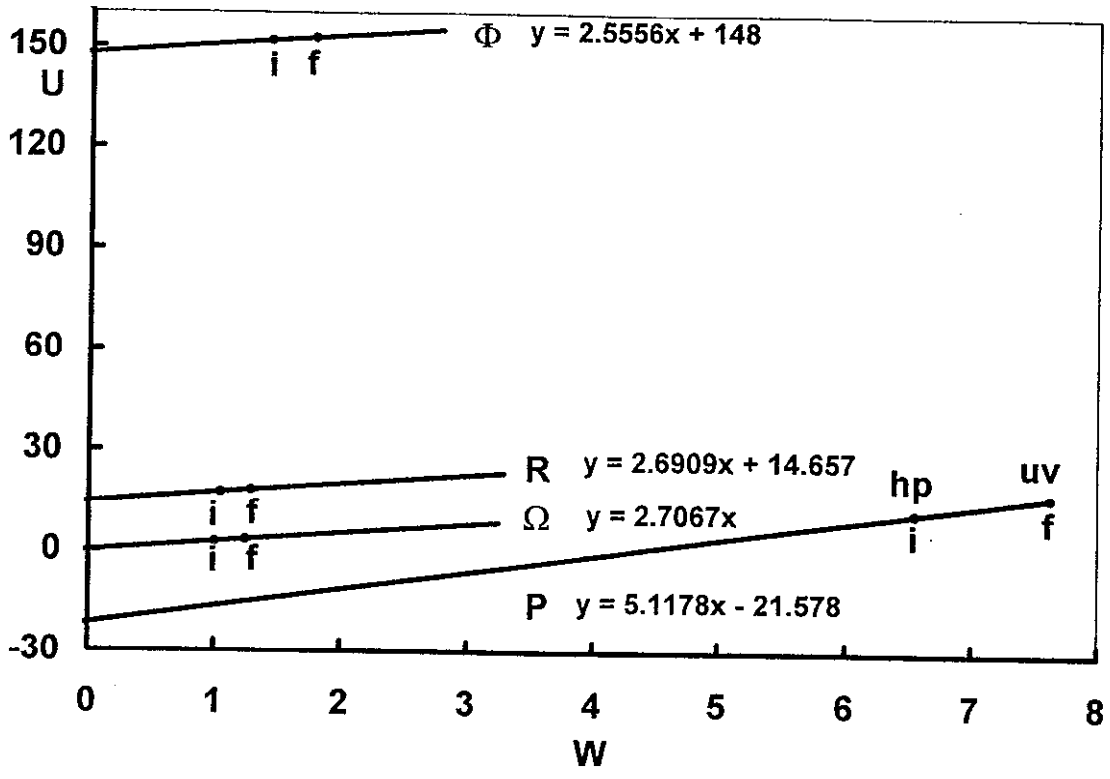

Figure 16. Le Chatelier diagram for confined combustion of TNT explosion products in air.

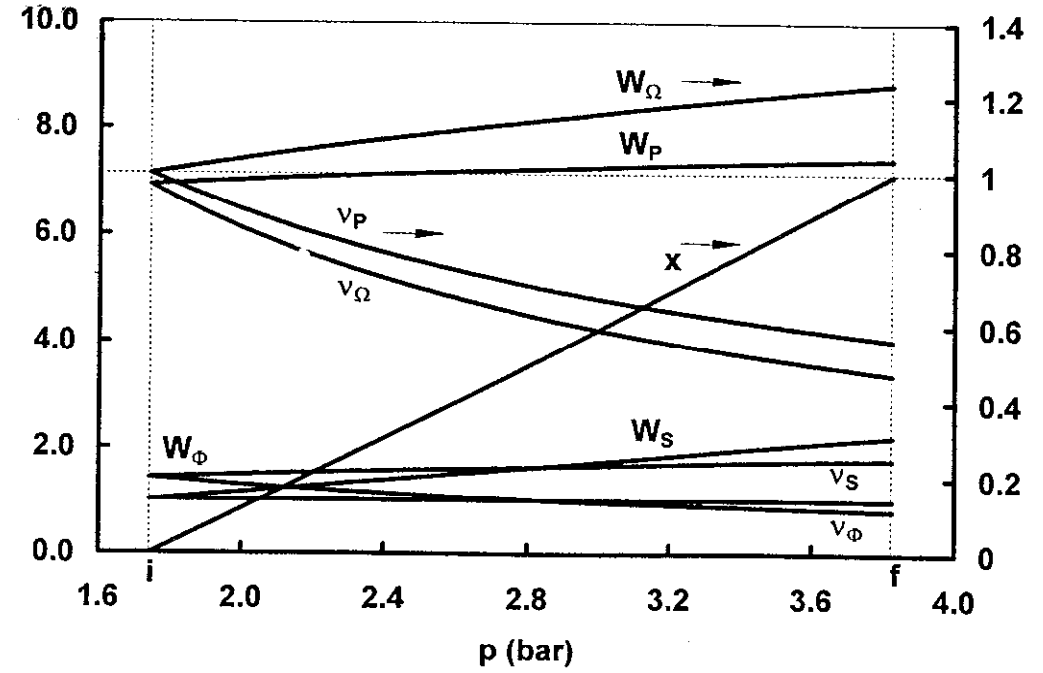

Figure 17. Profiles of thermodynamics parameters with respect to pressure.

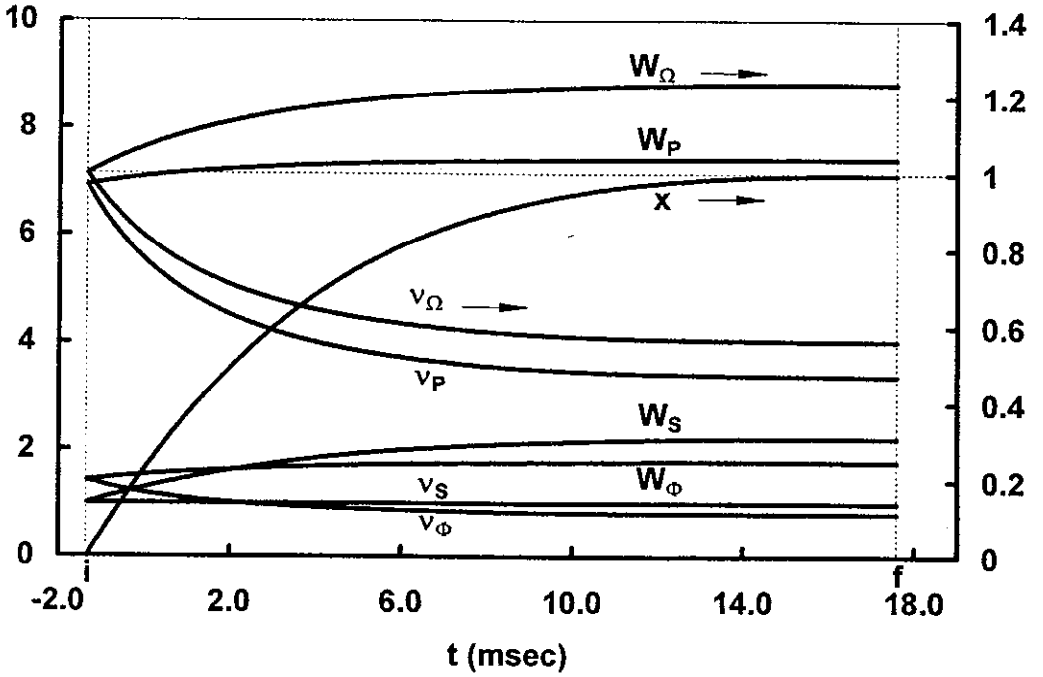

Figure 18. Profiles of thermodynamic parameters with respect to time.

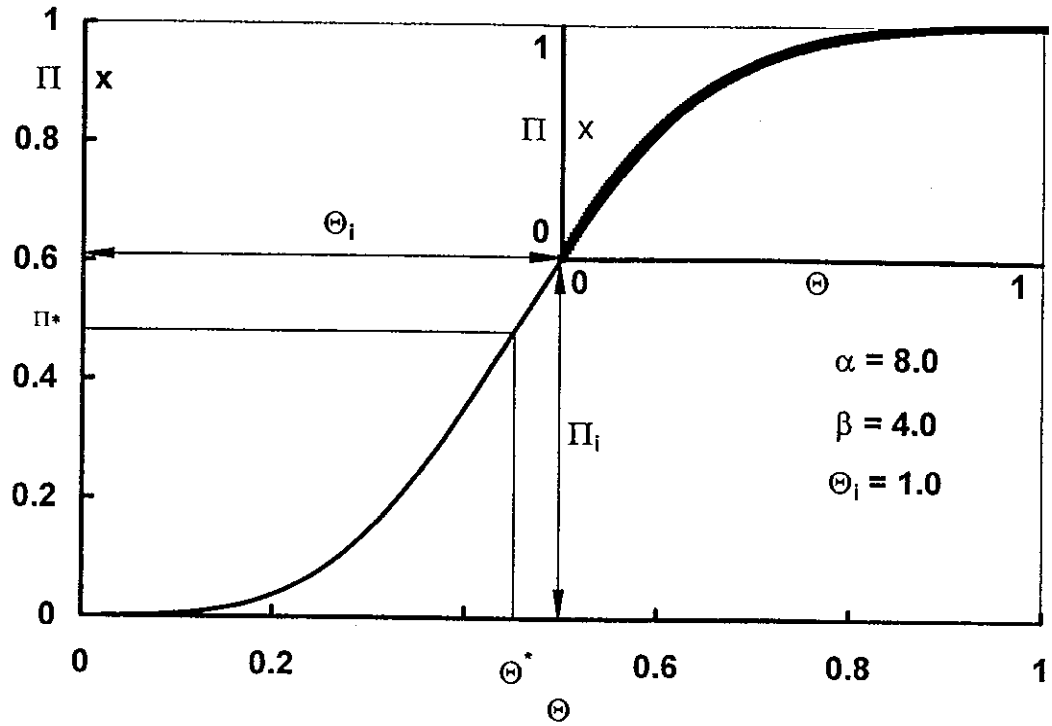

Figure 19. Dynamic properties of confined combustion of TNT explosion products in air.

Numerical Simulations

Based on the ideas Zel'dovich expressed *in The Mathematical Theory of Combustion and Explosions* [49] (especially Chapter 6), as well as Shchelkin and Troshin's concepts in *Gasdynamics of Combustion* [53], we have proposed a model of the process [60].

Formulation

The goal here is to simulate the fluid-dynamic aspects of the mixing and combustion of TNT explosion products with air in an enclosure. The products-air interface is unstable, and rapidly evolves into a turbulent mixing layer (vid. Kuhl [64]). As the products expand, they entrain air from the surroundings as a consequence of its large-scale vortical structures. Concomitantly, the exothermic process of combustion is associated with local deposition of exothermic energy—engendering dilatation. The mixing takes place in the turbulent velocity field of the hot combustion products, so that the oxidation rate is, in effect, controlled by the turbulent mixing rate (the chemical rates being virtually instantaneous under such conditions). The model is specified by the recognition that the flow field consists of three components: *fuel-F* (expanded TNT detonation products), *oxidizer-O* (air) and combustion *products-P*, at their final state of thermodynamic equilibrium. We consider the inviscid exothermic-flow limit [65]—where all molecular transport phenomena associated with viscosity, diffusion, conduction and finite reaction rates are disregarded. Hence, the Reynolds number $Re \to \infty$; the Peclet number for both heat and mass diffusion $Pe \to \infty$; the Damköhler number $Da \to \infty$, but, since compressibility effects are predominant, the Mach number: $Ma > 0$. As is typical of combustion in unmixed systems, the fuel reacts with the oxidizer in stoichiometric proportions.

Conservation Equations

In the limit of $Re \to \infty$, the mixture obeys the conservation equations of gasdynamics:

$$\partial_t \rho + \nabla \cdot (\rho \mathbf{u}) = 0 \tag{31}$$

$$\partial_t \rho \mathbf{u} + \nabla \cdot (\rho \mathbf{u}\mathbf{u}) = -\nabla p \tag{32}$$

$$\partial_t \rho E + \nabla \cdot (\rho E \mathbf{u}) = -\nabla \cdot (p\mathbf{u}) + Q_a \rho \langle Y_F \rangle_i \delta(t - t_i) \tag{33}$$

where ρ, e, p and $\mathbf{u}$ denote the mixture density, internal energy, pressure and velocity, respectively, while $E \equiv e + \mathbf{u}\cdot\mathbf{u}/2$. These equations are integrated with a high-order Godunov scheme first developed by Colella & Glaz [66]. Adaptive Mesh Refinement (AMR) , as formulated by Berger & Colella [67] and developed by Bell et al [68], is used to capture the energy-bearing scales of the turbulent flow on the computational grid. In analogy to non-reactive flows [69], we claim that a Godunov-based solution of the above equations determines a large Reynolds-number, convective-mixing approximation to the turbulent velocity field—which combustion influences solely through the exothermic power represented by the last term in Eq. (33).

Exothermicity

At the $Pe \to \infty$ limit considered here, the mass fractions $Y_k \equiv \rho_k / \rho$ (k =F, O, P) of the component fluids are governed by the following advection equations:

$$\partial_t Y_F + \mathbf{u}\cdot\nabla Y_F = -\dot{Y}_F = \langle Y_F \rangle_i \delta(t - t_i) \tag{34}$$

$$\partial_t Y_O + \mathbf{u}\cdot\nabla Y_O = -\dot{Y}_O = -\phi_s \dot{Y}_F = \phi_s \langle Y_F \rangle_i \delta(t - t_i) \tag{35}$$

$$\partial_t Y_P + \mathbf{u}\cdot\nabla Y_P = \dot{Y}_F + \dot{Y}_O = (1 + \phi_s)\langle Y_F \rangle_i \delta(t - t_i) \tag{36}$$

$$Y_F + Y_O + Y_P = 1 \tag{37}$$

where, for a TNT-air mixture, the stoichiometric coefficient is $\phi_s \equiv (m_{air} / m_{fuel})_s = 3.2$ (vid. Table 4). Combustion influences these fields by fuel-consumption at a rate of $\dot{Y}_F$. According to the approximation of $Da \to \infty$, source terms are implemented as Dirac delta functions, δ, whose strength is specified by the following heuristic rule for this unmixed system: *fuel and oxidizer cannot coexist under these conditions; whenever (i.e., at time t_i) and wherever (i.e., at cell $\mathbf{x}_i$) fuel and oxidizer are found in the same cell (i.e., $0 < \phi < \infty$), they instantly react in stoichiometric proportions to form combustion products* . Implemented as an algorithm, this rule is expressed as:

$$\langle Y_F \rangle_i \equiv \begin{cases} Y_F(\mathbf{x}_i, t_i) & (\phi_i \geq \phi_s) \\ Y_O(\mathbf{x}_i, t_i)/\phi_s & (\phi_i < \phi_s) \end{cases} \tag{38}$$

A Godunov-based solution of Eqs. (34)-(38) establishes, according to us, a large-Peclet-number, connective-mixing approximation to the behavior of component fluids in a turbulent velocity field, **u**.

Equations of state

The components were treated as a mixture of gases in thermodynamic equilibrium. Initially, (at high pressures/small expansions), the fuel was modeled by a Jones-Wilkins-Lee (JWL) equation of state for detonation products gases:

$$p_F = A(1 - w\rho_c / \rho R_1)e^{-R_1\rho_c/\rho} + B(1 - w\rho_c / \rho R_2)e^{-R_2\rho_c/\rho} + w\rho e \qquad (39)$$

where A = 3.712 Mbars, B = 0.03231 Mbars, R_1 = 4.15, R_2 = 0.95, and $w = (\gamma_F - 1)$ =1.30 for TNT (Dobratz [70]). Later, the thermodynamic model (previous section) was used:

$$p_F = (\gamma_F - 1)\rho_F e_F \quad \text{with } \gamma_F = 1.39 \;\&\; e_F = w_{\Omega i}(U_\Phi - 148) \qquad (40)$$

$$p_O = (\gamma_O - 1)\rho_O e_O \quad \text{with } \gamma_O = 1.37 \;\&\; e_O = w_{\Omega i}U_\Omega \qquad (41)$$

$$p_P = (\gamma_P - 1)\rho_P e_P \quad \text{with } \gamma_P = 1.20 \;\&\; e_P = w_{\Omega i}(U_P + 21.578) \qquad (42)$$

where $[p]$ = kJ/cc, $[\rho]$ = g/cc, $[e]$ = kJ/g and $w_{\Omega i} = 0.1281$ kJ/g $= 0.1281\times10^{10}$ erg/g. In mixed cells, the pressure was defined by a mass-weighted average.

Initial conditions

A schematic of the computational domain for the two-dimensional (2-D) simulations is shown in Fig. 20. It consisted of a cylindrical tank with radius of 117 cm and half-length of 193.5 cm (corresponding to the explosion chamber volume of V = 16.6 m^3). Only one quadrant of the domain (indicated by the solid lines) was calculated. Consistent with the inviscid flow assumption, slip-flow boundary conditions were used on the walls (i.e., at r = 117 cm and at z = 193.5 cm), while symmetry boundary conditions were used at the axis of r = 0 and on the surface z = 0. Two levels of Adaptive Mesh Refinement (AMR) were used, with a base grid mesh size of $\Delta_1 = 0.5$ cm and a fine mesh size of $\Delta_2 = 0.25$ cm. With this zoning, the 2-D calculations took 125 hours CPU time on a *J90* computer to simulate 28 ms of the problem.

Three-dimensional (3-D) simulations were performed in a cube of half-dimension of 151.6 cm (V = 16.6 m^3). Only a one-eighth segment of the problem was calculated. Again, slip-flow boundary conditions were used on the walls (i.e., at x = 151.6 cm, at y = 151.6 cm and at z = 151.6 cm), while symmetry boundary conditions were used on the

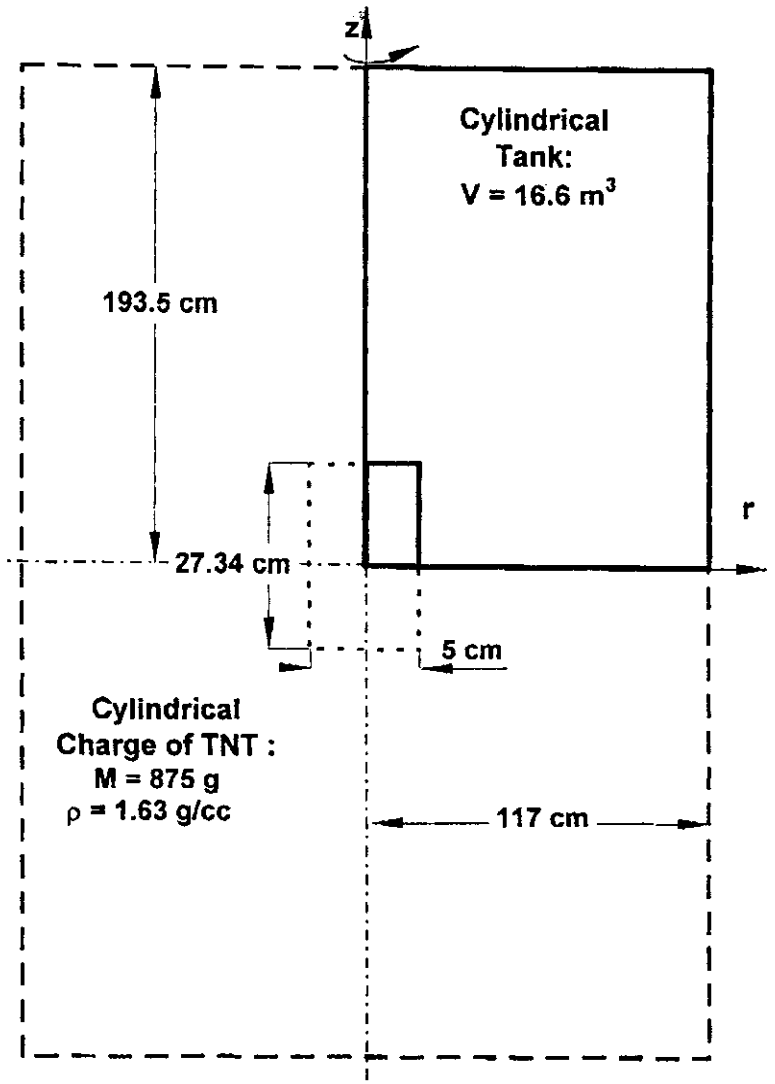

Figure 20. Schematic of the computational domain: 2-D simulations.

planes x=0, and y=0, and z=0. Again, two levels of refinement were used, with a base grid mesh size of $\Delta_1 = 2$ cm and a fine mesh size of $\Delta_2 = 1$ cm. With this zoning, the 3-D calculations took 200 hours CPU time on a *J90* computer to simulate 28ms of the problem.

The initial atmosphere in the chamber was taken as quiescent air at sea-level conditions:

$$\rho_O = 1.2254 \times 10^{-3} \text{ g/cm}^3, e_O = 1.94 \times 10^9 \text{ erg/g}, p_O = 1.01325 \times 10^6 \text{ dy/cm}^2,$$

$$a_O = 3.34 \times 10^4 \text{ cm/s, and } \mathbf{u}_O = 0.$$

A cylindrical TNT charge (radius $R_c = 2.5$ cm, length l=27.34 cm) with mass of $m_c = 875$ g and density of $\rho_c = 1.63$ g/cm^3, was placed at the center of the domain (Fig. 20). We assumed that the charge was detonated by a line source at $r = 0$. This initiated a cylindrical Chapman-Jouguet (CJ) detonation wave. According to Dobratz [70], the CJ parameters for TNT are: $p_{CJ} = 210$ kbars, $\rho_{CJ} = 2.23$ g/cm^3, $e_{CJ} = 6.02 \times 10^{10}$ erg/g, $u_{CJ} = 1.86$ km/s, and $\Gamma_{CJ} = 2.727$, with a corresponding detonation velocity $D_{CJ} = 6.93$ km/s and heat of detonation $q_{CJ} = 4.29 \times 10^{10}$ erg/g.

When the wave reached R_c, the flow field corresponding to a one-dimensional cylindrical CJ detonation wave (Taylor [71], Sedov [72], Zel'dovich & Kompaneets [27]) was mapped onto the the computational domain. Thus, an initial value problem was formulated, with gaseous products of TNT detonation expanding into air. Results are described in the next section.

Results

A cinematic visualization of the numerical simulation is presented in Fig. 21. It depicts the detonation of the cylindrical TNT charge, the expansion of the detonation products gases and their mixing with the surroundings, and the combustion of the explosion products with air. Component fluids are represented by colors: *yellow* fuel (TNT explosion products) mixes with *blue* oxidizer (air) forming *red* combustion products. The accompanying color bar, is, in effect, a graphical representation of the Shavb [74]-Zel'dovich [75] variable: $Y \equiv Y_O - \phi_s Y_F$. Exothermic cells are marked by white dots. Shown also on the diagram are overlays of gray vorticity contours and black dilatation contours—to illustrate the coupling between fluid mechanics and exothermicity.

The blast wave from the cylindrical charge was very directional. A "cylindrical" blast wave expanded radially from charge, while a "jet-driven" blast wave propagated

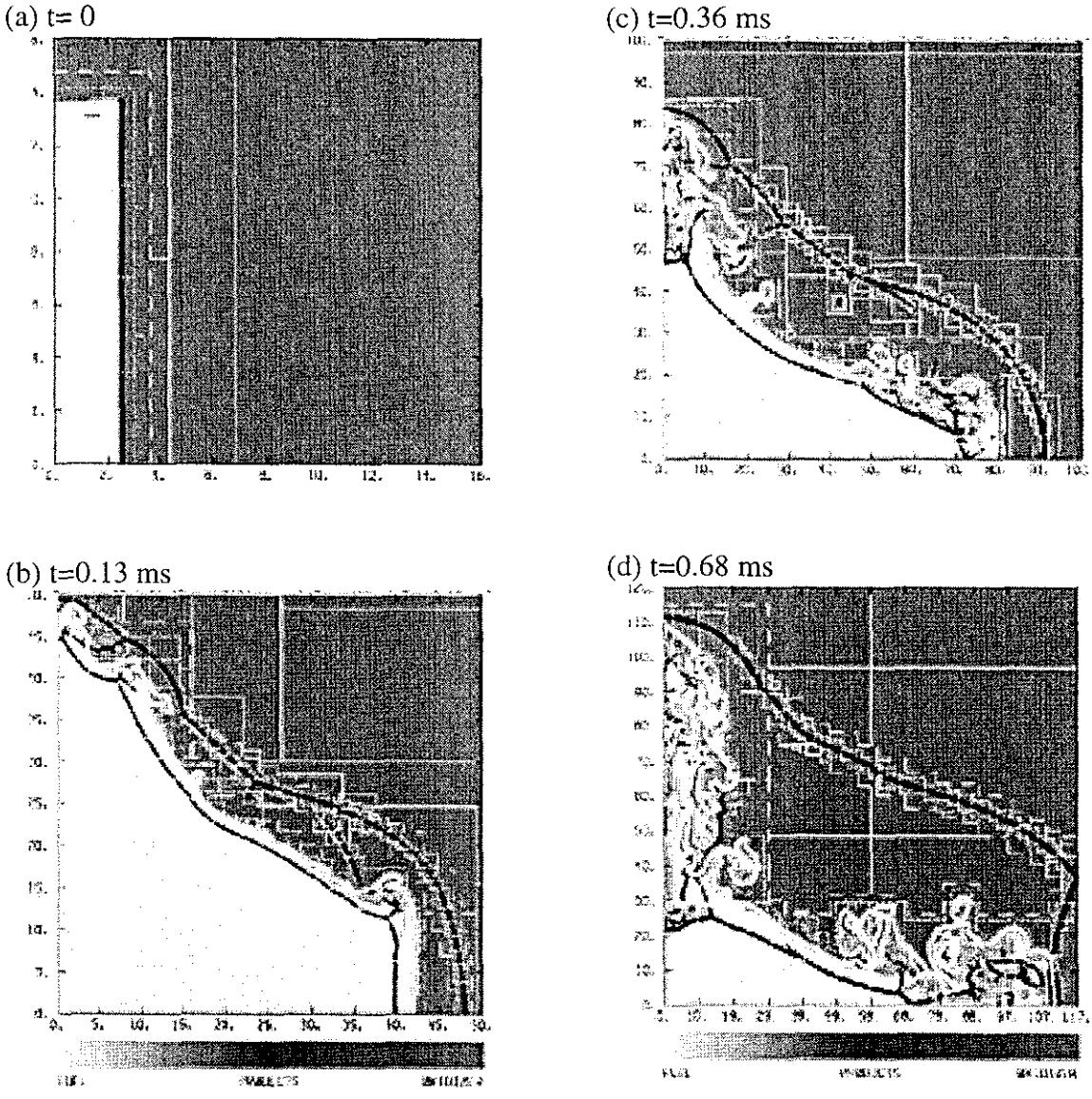

Figure 21. AMR simulation of the explosion on a 875-g cylindrical TNT charge in a 16.6-m^3 chamber filled with air at atmospheric pressure. TNT explosion products (shown in *yellow*), mix with oxidizer (depicted as *blue*), thereby forming combustion products (represented as *red*). Exothermic cells are marked by white dots. Vorticity contours are *gray*, while dilatation contours are *black*. Times are listed in milliseconds.

(e) t=1.0 ms

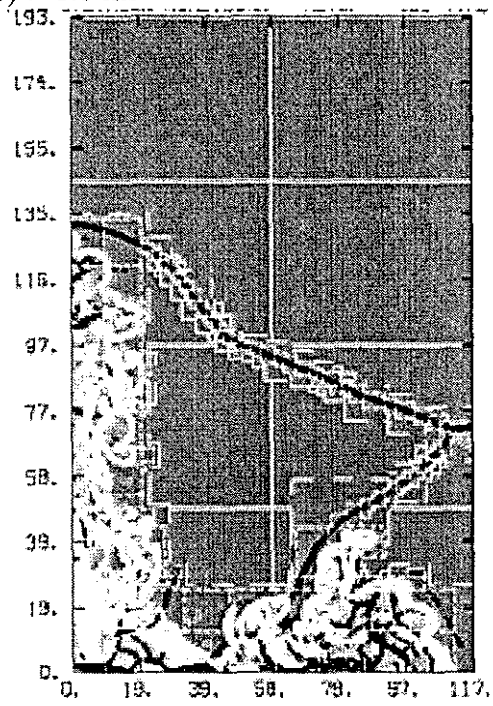

(g) t=3.0 ms

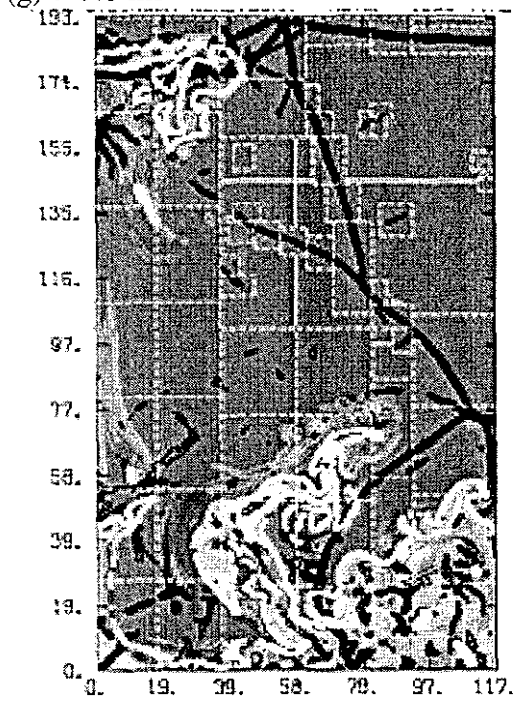

(f) t=2.0 ms

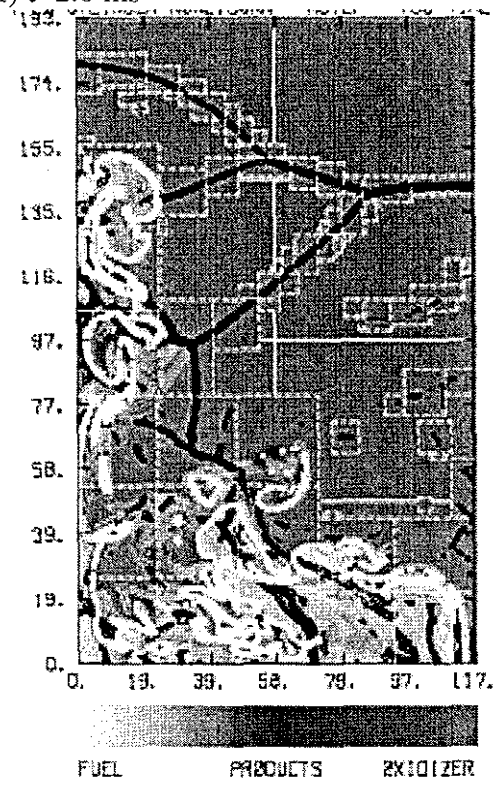

(h) t=3.8 ms

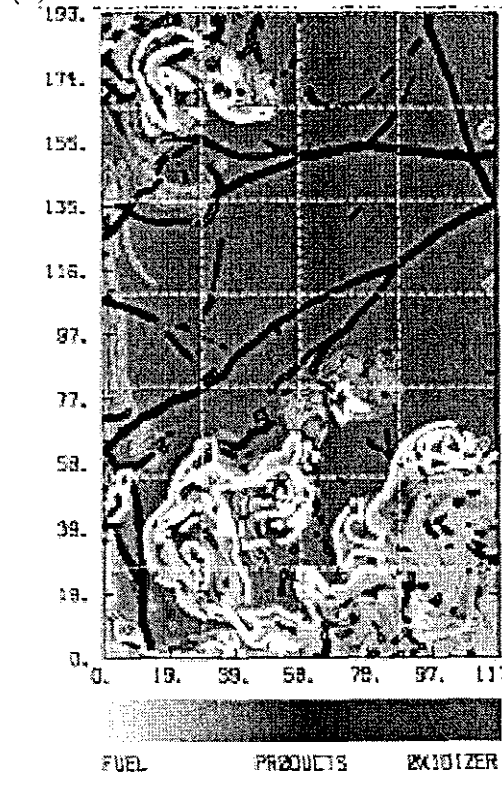

Figure 21: continued

(i) t=4.7 ms

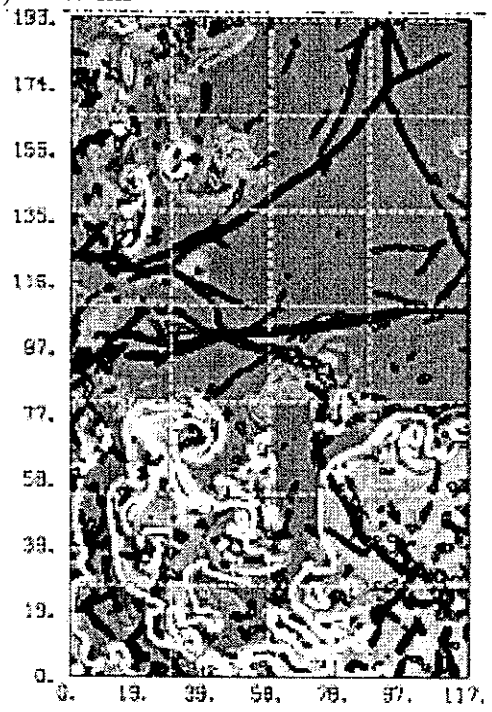

(k) t=6.6 ms

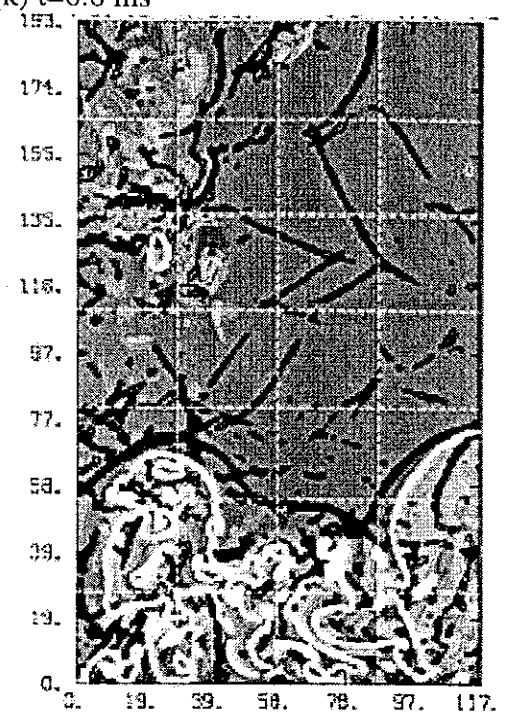

(j) t=5.7 ms

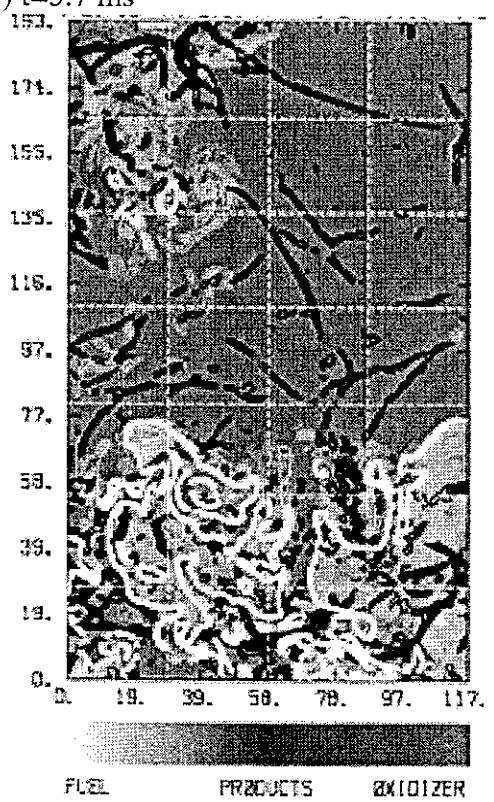

(l) t=7.5 ms

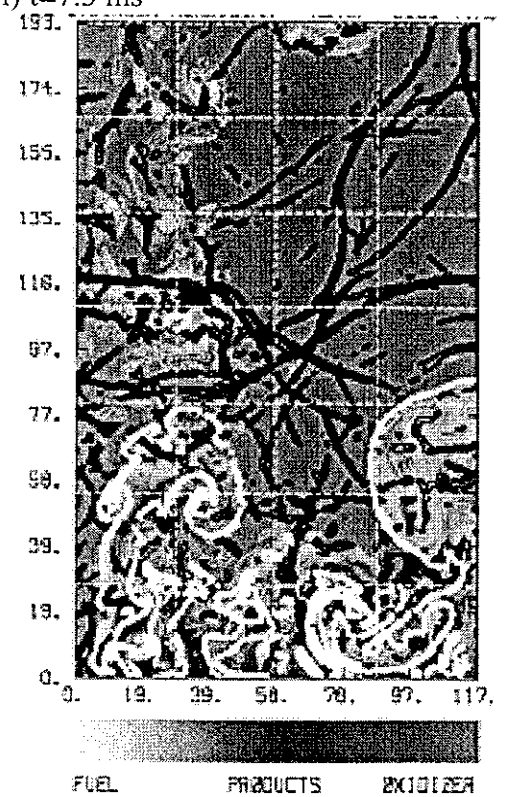

Figure 21: continued

(m) t=10.2 ms

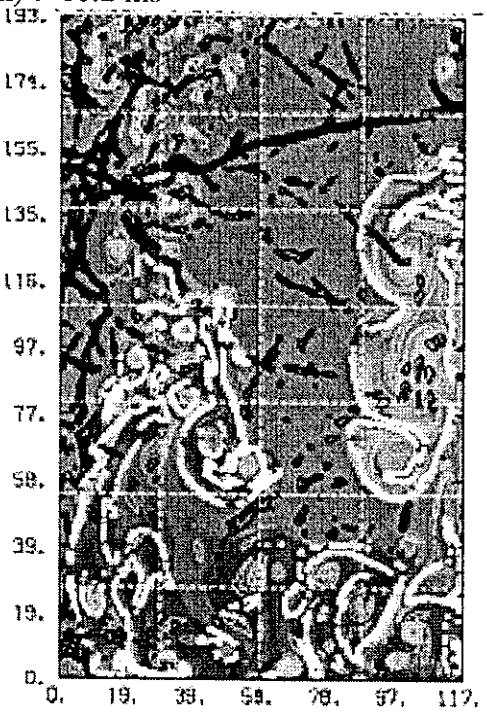

(o) t=19.7 ms

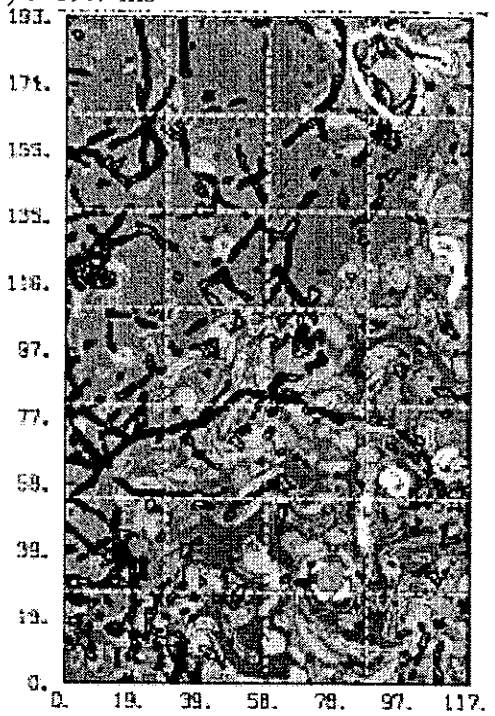

(n) t=14.5 ms

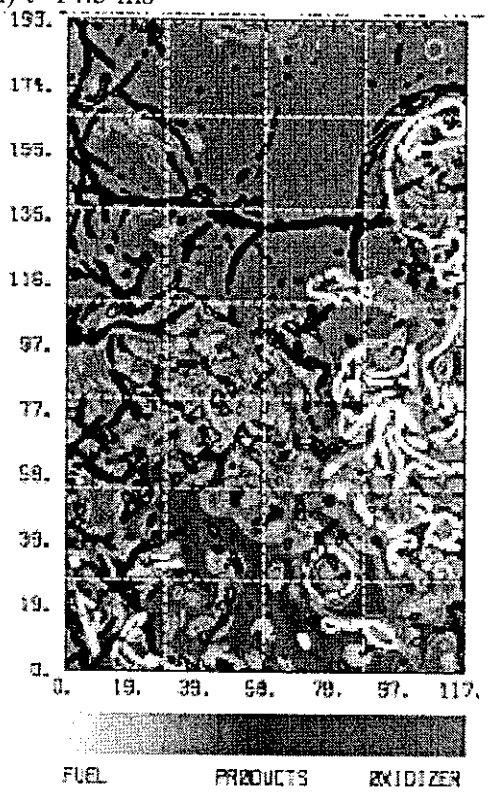

(p) t=28.1 ms

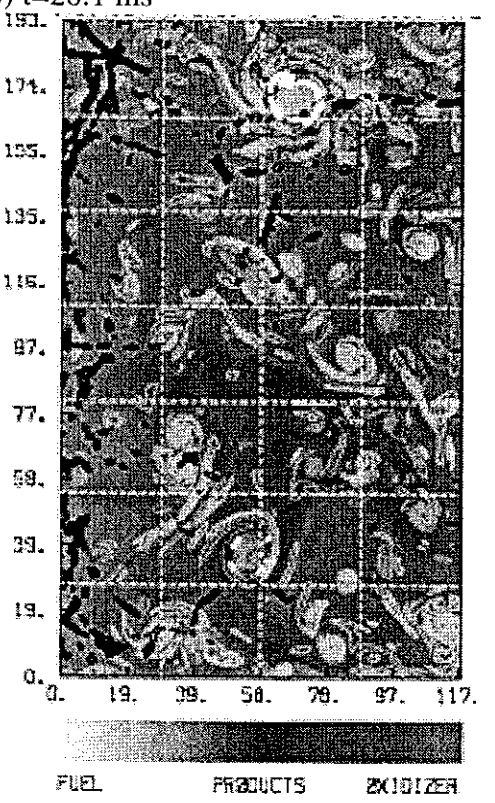

Figure 21: concluded

along the charge axis. Thus, the TNT explosion products formed a "cross-shaped" volume, as observed in recent experiments*. The "cylindrical" portion of the blast wave reflected from the side wall of the chamber at $t \cong 0.65$ ms, while the "jet" portion reached the end wall at $t \cong 2$ ms.

The TNT-air interface was accelerated by a strong shock (a 210-kbar detonation wave); it was therefore susceptible to Richtmyer [76]-Meshkov [77] instabilities, and rapidly evolved into a turbulent mixing layer (vid. Anisimov and Zel'dovich [78], Anisimov et al [79], Kuhl [64]). Large-scale rotational structures caused air to be rapidly entrained into the fuel cloud; fine-scale structures caused intense local mixing—leading to rapid combustion. Initially ($t < 0.5$ ms), energy deposition occurred in a thin exothermic sheet near the fuel boundary. Later ($t > 1$ ms), these exothermic sheets became distributed throughout the fuel cloud due to the turbulent field—thereby exhibiting the "distributed combustion mode" described by Peters [80], and by Liñán & Williams [81]. Most of the fuel mass was concentrated in a "donut-shaped" region near the chamber wall—where most of the energy deposition occurred.

Static pressure histories at the side wall of the chamber are presented in Fig. 22. Results of the AMR simulations are in excellent agreement with the experimental measurements—indicating that exothermic model employed here captures the dominant energy release mechanism for such flows.

The fuel mass-fraction burned, as deduced from the 3-D AMR simulations, is depicted in Fig. 23. Burning starts on an exothermic surface of finite area (the charge surface), so the curve starts with a finite slope (in contrast to weak ignition from a point, which exhibits an "S-shaped" burning curve). Most of the fuel is consumed during the first 15 ms, with the remaining 10% being consumed over much longer times (15-30 ms).

Conclusions

Detonation of a TNT charge creates a hot gaseous "fuel" that is rich in carbon dust and carbon dioxide. When this fuel mixes with air due to turbulence in the explosion field, rapid combustion (after-burning) occurs. For TNT, this combustion energy is about three times larger than the heat of detonation (i.e., 3,500 Cal/g versus 1,000 Cal/g, respectively). For confined explosions, this combustion effect is manifested

* Dr. H. Reichenbach, Ernst Mach Institut, Freiburg, Germany (private communication).

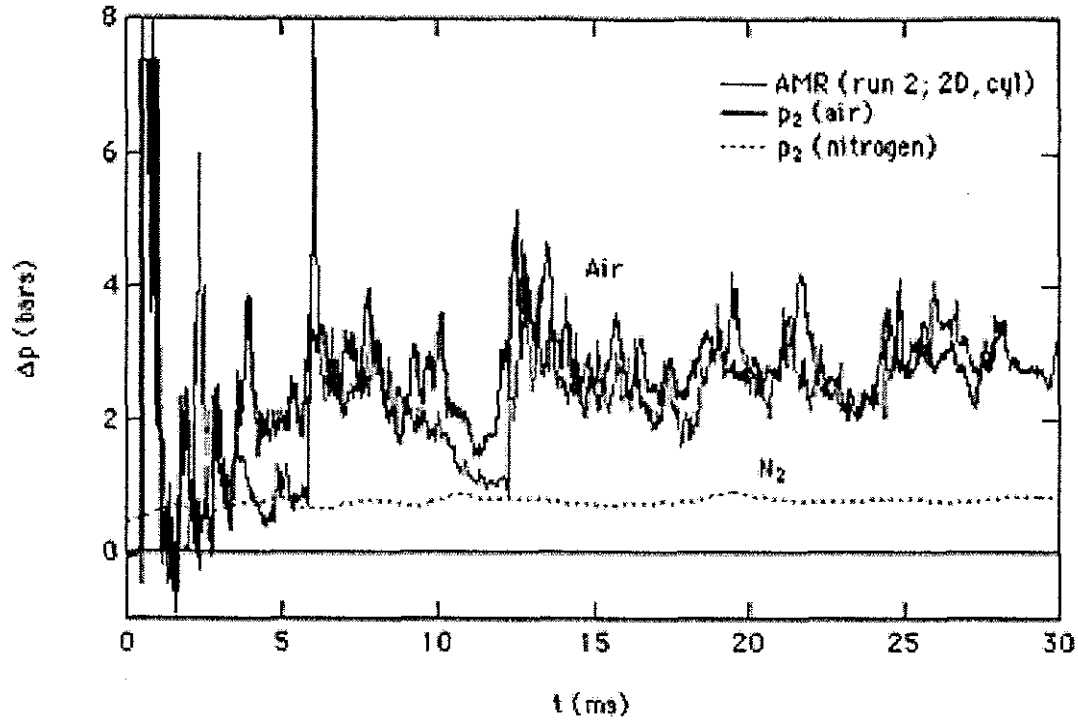

Figure 22. Over-pressure history from the AMR simulation of a TNT explosion and combustion in air compared with TNT experiments in air (test #3, gauge 2) and nitrogen (test #1, gauge 1) atmospheres.

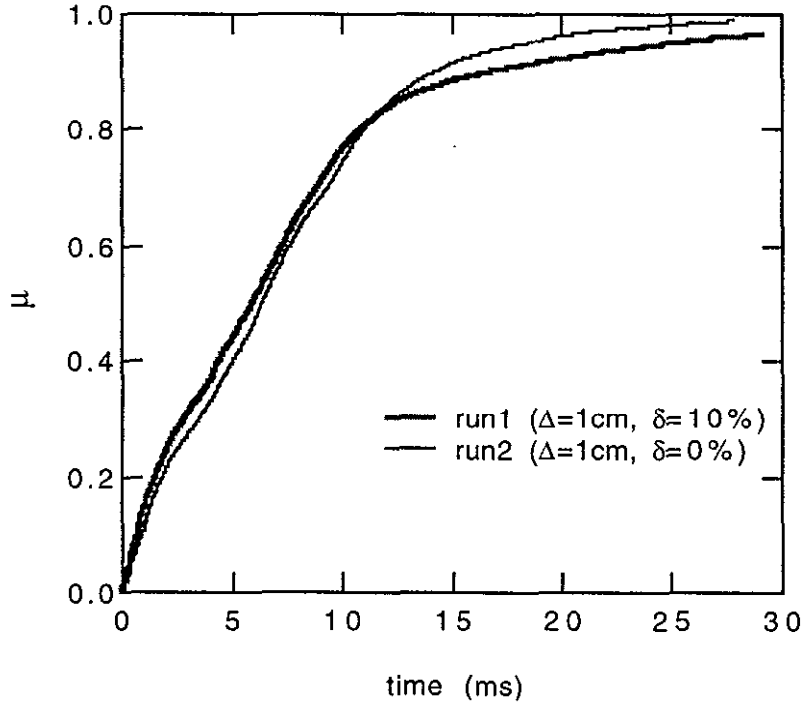

Figure 23. Mass-fraction burned from 3D AMR simulations of turbulent combustion of TNT products in air (875 g charge in a16.6-m^3 chamber).

by a three-fold increase in the mean pressure in the enclosure. Experiments performed with 0.8 kg charges of TNT and TRITONAL conclusively demonstrate this effect.

A thermodynamic analysis of the closed combustion process was developed, based on four principles: (i) thermodynamic properties of the components; (ii) balance of mass; (iii) balance of volume; (iv) balance of energy. The first provides the functional relationship between the internal energies, $\mathbf{u}_K$, and the corresponding thermodynamic reference parameters, $\mathbf{w}_K \equiv \mathbf{p}_K \mathbf{v}_K$ ($K = \Phi, \Omega, R, P$)—thereby eliminating $\mathbf{u}_K$ from further relationships. The second permits the mass fractions of all the components to be expresses in terms of one of the $\mathbf{Y}_K$, namely $\mathbf{Y}$. The third furnishes an expression for $\mathbf{w}_P$ in terms of the reference parameters of the reactants and $\mathbf{Y}$. On this basis, the fourth yields $\mathbf{Y} = \mathbf{Y}(\mathbf{w}_\Phi, \mathbf{w}_\Omega)$ or $\mathbf{Y} = \mathbf{Y}(\mathbf{w}_R)$, and the expression used to eliminate $\mathbf{w}_P$ is then utilized to determine its value. The reference parameters of the reactant species are then expressed in terms of pressure. The coordinates of $\mathbf{w}_K$ ($K = \Phi, \Omega$) are finally expressed in terms of pressure by means of polytropic relations. Thus, in the absence of energy loss by heat transfer to the walls (which turned out to be here the case), the mass fraction of fuel consumed by the exothermic process of combustion becomes solely a function of pressure. Upon this background, dynamic features of the exothermic process become expressible in terms of a normalized constrained exponential function, and all their properties are described concisely by three parameters of this function: α, β, Θ_i.

The experiments were modeled as a turbulent combustion in an unmixed system at infinite Reynolds, Peclet and Damköhler numbers. The governing conservation laws were integrated by a high-order Godunov scheme; AMR was used to capture the energy-bearing scales of the turbulent mixing on the computational mesh. The calculated pressure histories were in good agreement with experimental measurements—indicating that exothermic model employed here captures the dominant energy deposition mechanism for such flows. Based on these simulations, most (>90%) of the fuel (TNT explosion products) was consumed in about 15 ms, for a 0.875-kg TNT charge detonated in a 16.6-m^3 chamber. The model elucidates the dynamics of turbulent combustion under circumstances where exothermic effects are controlled by fluid dynamics of the turbulent field [65], rather than by a reaction-diffusion mechanism, typical of laminar flames. Provided thus is an example of a highly-turbulent combustion field—a regime of exothermic flow that is still relatively unexplored despite its practical significance.

Acknowledgements

This work was performed under the auspices of the U. S. Department of Energy by the Lawrence Livermore National Laboratory under Contract number W-7405-ENG-48. This research was also sponsored by the Defense Special Weapons Agency under DSWA IACRO #98-3016.

References

Historical Developments

[1] Assehton, R., *History of Explosives*, 2nd Ed., Institute of Makers of Explosives, New York, 1940.

[2] Schönbein, C.F. "Sitzungs Berichte der Naturforscher Gesellschaft", Basel, **7**, 1846, p. 26; US Patent 4674, 1846.

[3] Sobrero, A., "Sur Plusieurs Composés Detonants Produits avec l'Acide Nitrique et le Sucre, le Dextrine, la Lactine, la Marnite, et la Glycérine", *Comptes-Rendus Académie des Sciences*, Paris, **25**, 1847, pp. 247-248.

[4] Abel, F.A., "Contribution to the History of Explosive Agents", *Philosophical Transactions*, **159**,1869, pp. 489-516; also *Comptes-Rendus Academie des Sciences*, Paris, **69**, 1869, pp. 105-121.

[5] Nobel, A. and Abel, F. A., "Researches on Explosives", *Philosophical Transactions Royal Society of London*, **165**, 1875, pp. 129-237; **171**, 1880, p. 204.

[6] Berthelot, M., "Sur la Vitesse de Propagation des Phenomènes Explosifs dans les Gaz", *Comptes-Rendus Académie des Sciences*, Paris, **93**, 1881, pp. 18-22; "Sur l'Onde Explosive", *Comptes-Rendus Académie des Sciences*, Paris, **94**, 1882, pp. 149-152.

[7] Berthelot, M., and Vieille, P., "'Personal Investigations' of the Members of the French 'Commission des Substances Explosives'", *Memorial des Poudres et Salpêtres*, **1**, 1878-1883, p. 462.

[8] Mallard, E., and Le Chatelier, H., "Sur la Vitesse de Propagation de l'Iflammmation dans les Mélanges Gazeux Explosifs," *Comptes-Rendus Académie des Sciences*, Paris, **93**, 1881, pp. 145-148; "Recherches sur la Combustion des Mélanges Gazeux Explosifs", *Annales des Mines*, 8e Serie, **4**, 1883, pp. 274-568, 10 PLATES/VIII-XVII.

[9] Hugoniot, H., "Propagation des Mouvements dans les Corps et spécialement dans les Gaz Parfaits", *Journal de l'Ecole Polytechnique*, Cahiers, **57**, 1887, p. 3; **58**, 1889, p. 1.

[10] Munroe, C. E., "Wavelike Effects Produced by the Detonation of Guncotton", *American Journal of Science*, **36**, p. 48, 1888.

[11] Chapman, D. L., "On the Rate of Explosion in Gases", *London-Edinburgh-Dublin Philosophical Magazine*, **47**, p. 90, 1899.

[12] Dixon, H., "The Rate of the Flame in the Explosion of Gases", *Philosophical Transactions A*, **184**, 1903, pp. 97-188; "The Rate of Flame Propagation in the Explosion of Gases", *Philosophical Transactions* A, **200**, 1903, pp. 315-351.

[13] Jouguet, E., "Sur la Propagation des Réactions Chimiques dans les Gaz", *Journal des Mathématiques Pures et Appliquées*, 6th Serie, 1905-1906, **1**, p. 347; **2**, p. 5; *La Mécanique des Explosifs*, O. Doin Publisher, Paris, 1917.

[14] Bauer, P. A., Dabora, E.K., Manson, N., "Chronology of Early Research on Detonation Waves", *Dynamics of Detonations and Explosions: Detonations*, Edited by A. L. Kuhl, J.-C. Leyer, A. A. Borisov, and W. A. Sirignano, *Progress in Astronautics and Aeronautics*, **133**, AIAA, Washington DC, 1991, pp. 3-18.

[15] Manson, N. and Dabora, E. K., "Chronology of Research on Detonation Waves: 1920-1950", *Dynamic Aspects of Detonations*, , Edited by A. L. Kuhl, J.-C. Leyer, A. A. Borisov, and W. A. Sirignano, *Progress in Astronautics and Aeronautics*, **153**, AIAA, Washington DC, 1993, pp. 3-39.

Monographs on Condensed Explosives

[16] Marshall, A., *Explosives*, P. Blakiston's Sons & Company, Philadelphia, 1917.
[17] Taylor, J., *Detonation in Condensed Explosives*, University Press, Oxford, xi + 196 pp. + x plates, 1952.

[18] Bowden, F. P., and Yoffe, A., *Initiation of Explosives*, University Press, Cambridge, 1952.

[19] Cook, M. A., *The Science of High Explosives*, American Chemical Socicty Monograph **139**, Reinhold Publishing Corp, New York, Chapman & Hall Ltd., London, xv + 440 pp., 1958.

[20] Taylor, W., *Modern Explosives*, The Royal Institute of Chemistry, London, Monograph **5**, 1959.

[21] Belyaev, A. F., *Combustion, Detonation and Explosion Work of Condensed Systems*, USSR Academy of Sciences, Moscow, 1968.

[22] Johansson, C. H., and Persson, P. A., *Detonics of High Explosives*, Academic Press, London, xiii + 330 pp., 1970.

[23] Fickett, W., and Davis, W. C., *Detonation*, University of California Press, Berkeley, xiv + 386 pp., 1979.

[24] Mader, C.L., *Numerical Modeling of Detonation*, University of California Press, Berkeley, x + 485 pp., 1979.

[25] Cheret, R., *Detonation of Condensed Explosives*, Springer Verlag, New York, xxii + 427 pp., 1993.

[26] von Neumann, J., Theory of Detonation Waves, in *John von Neumann Collected Works*, Vol. **6**, ed. A. J. Taub, MacMillan, New York, {originally OSDR Report **549**, 1942}.

[27] Zel'dovich, Ya. B, and Kompaneets, A. S., *Theory of Detonation*, Academic Press, New York, 284 pp., 1960 (originally published in Moscow in 1955).

[28] Grushka, H. D., and Wecken, F., *Gasdynamic Theory of Detonation*, Gordon and Breach, New York, xii + 198 pp., 1971.

[29] Nettleton, M. A., *Gaseous Detonations: their nature, effects and control*, Chapman & Hall Publishers, London, xiv + 255 pp., 1987.

[30] Persson, P-A., Holmber, R., and Lee, J., *Rock Blasting and Explosives Engineering (a textbook for students and a handbook for scientists and engineers covering the science and engineering of the industrial use of explosives with major emphasis on rock blasting)*, CRC Press, Boca Raton, Florida, 3rd printing, 540 pp., 1996.

Journal Articles on TNT

[31] Goranson, R. W., *Method of Determining Equation of State and Reaction Zones in the Detonation of High Explosives, and its application to Pentolite, Composition B, Baratol, and TNT*, Los Alamos Scientific Laboratory, Report **LA-487**, 1946.

[32] Cybulski, W. B., Payman, W, and Woodhead, D.L., "Explosion waves and shock waves: VII. The velocity of detonation in cast TNT", *Proc. Roy. Soc. London*, A, **197**, pp. 51-72, 1949.

[33] Becker, R. "Stosswelle und Detonation", *J. Phys*, **8**, p. 321, 1922.

[34] Gawthrop, D. B., Shepherd, W. C. F., Perrot, G., "Photography of Waves and Vorticities Produced by the Discharge of an Explosive", *J. Franklin Inst.*, **211**, 67, p. 401, 1931.

[35] Ihyukhin,V.S., Pokhil, P.E., Rozanov, D.K., and Shvedova, N.S., "Measurement of the Shock Adiabate for Cast TNT, Crystalline RDX, and Nitromethane", *Dokl. Acad. Nauk SSSR* **131**, p. 793, 1960 {english trans. *Soviet Phys. Dokl.*, **5**, p. 337}.

[36] Garn, W. B., "Detonation Pressure of Liquid TNT", *J. Chem Phys.*, **32**, p. 653, 1960.

[37] Urizar, M.J., James, E. Jr., and Smith, L.C., "Detonation Velocity of Pressed TNT", *Physics of Fluids*, **4**, 1961, pp. 262.

[38] Kamlet, M. J., and Jacobs, S. J., "Chemistry of Detonations: I. A Simple Method of Calculating Detonation Properties of C-H-N-O based Explosives", *J. Chem. Phys.* **48**, pp. 23-25, 1968.

Combustion

[39] Weinberg, F. J. "The First Half-Million Years of Combustion Research and Today's Burning Problems", *Fifteenth Symposium (Int.) on Combustion*, Combustion Institute, Pittsburgh, Pennsylvania (1974), pp. 1-17.

[40] Jost, W., *Explosion and Combustion Processes in Gases*, translated by H. O. Croft, McGraw-Hill, New York (1946), xv + 621 pp {vid. especially Ch. IV: "Explosions in Closed Chambers", pp. 136-159, including the Mache effect}.

[41] Lewis, B. & von Elbe, G. *Combustion, Flames and Explosions of Gases*, (esp. Ch. V: Combustion Waves in Closed Vessels, pp. 381-395), Third Edition (1987), xxiv + 739 pp., Academic Press, Orlando, Florida.

[42] Williams, F. A. *Combustion Theory*, (Second Ed.) Benjamin/Cummings, Menlo Park, California, (1985), xxiii + 680 pp.

[43] Markstein, G. H., *Nonsteady Flame Propagation*, Pergamon Press Book, Macmillan, New York (1964), x + 328 pp.

[44] B. Lewis, R. N. Pease and H. S. Taylor Editors, *Combustion Processes*, Vol. **2**: *High-Speed Aerodynamics and Jet Propulsion*, Princeton University Press, Princeton, New Jersey (1956), xv + 662 pp.

[45] Semenov, N. N., *Tsepnye Reaktzii* (in Russian), Goskhimizdat, Leningrad (1934); *Chemical Kinetics and Chain Reactions*, Oxford at the Clarendon Press, Oxford (1935), xxii + 480 pp.

[46] Semenov, N. N., *Some Problems in Chemical Kinetics*, Translated by M. Boudart, Princeton University Press, Vol. 1 (1958), 239 pp.; Vol. 2 (1959), 331 pp.

[47] Zel'dovich, Ya. B., *Teoriya Goreniya i Detonatsii Gazov* (*Theory of Combustion and Detonation of Gases*), Acad. Nauk USSR, Moscow-Leningrad, (1944), 71 pp.

[48] Zel'dovich, Ya. B., and Frank-Kamenetzkii, D. A., "A Theory of Thermal Propagation of Flame", *ACTA Physico-Chimica URSS*, Vol. 9, No. 2 (1938), pp. 341-350.

[49] Zel'dovich, Ya. B., Barenblatt, G. I., Librovich, V. B., and Makhviladze, G. M., *The Mathematical Theory of Combustion and Explosions*, trans. by D. H. McNeill, Consultants Bureau of Plenum Publishing, New York (1985), xxi + 597 pp {vid. esp. Ch. 6: "Gasdynamics of Combustion", pp. 450-452}.

[50] Frank-Kamenetskii, D. A., *Diffusion and Heat Transfer in Chemical Kinetics*, (Second Ed.), translated by J. P. Appleton, Plenum Press, New York, (1969), xxvi + 574 pp.

[51] Kondrat'ev, V. N., *Chemical Kinetics of Gas Reactions*, translated by J. M Crabtree and S. N. Carruthers, edited by N. B. Slater, Pergamon Press, Oxford, Addison-Wesley Publishing, Reading, MA (1964), xii + 812 pp.

[52] Sokolik, A. S., *Self-Ignition, Flame and Detonation in Gases*, translated by N. Kaner, edited by R. Hardin, NASA TT F-125, OTS 63-11179 (1963), vi + 458 pp.

[53] Shchelkin, K. I., and Troshin, Ya. K., *Gasdynamics of Combustion*, trans. by B. W. Kuvshinoff and L. Holtschlag, Mono Book Corp., Baltimore, MA (1965), x + 222 pp.

Explosions

[54] Ornellas, D. L., Calorimetric Determination of the Heat and Products of Detonation for Explosives: October 1961 to April 1982, Lawrence Livermore National Laboratory, **UCRL-52821**, Livermore, CA, 1982.

[55] Fried, L. E., *CHEETAH 1.22 User's Manual*, **UCRL-MA-117541** (rev. 2), Lawrence Livermore National Laboratory, Livermore, CA, 187 pp., 1995.

[56] Dewey, J. M., "The Air Velocity in Blast Waves from TNT Explosions", *Proc. Roy. Soc. A*, **279**, 1964, pp. 366-385.

[57] Cudzilo, S., Paszula, J., Trebinski, R., Trzcinski, W., and Wolanski, P., "Studies of Afterburning of Detonation Products in Confined Explosions", *International Symposium on Hazard, Prevention, and Mitigation of Industrial Explosions—HPMIE*, in conjunction with: *Eighth International Colloquium on Dust Explosions*, Schaumberg, Illinois, September 21-25, 1998, 18 pp.

[58] Oppenheim, A. K., and Maxson, J. A., "Thermodynamics of Combustion in an Enclosure", *Dynamics of Heterogeneous Combustion and Reacting Systems*, Edited by A. L. Kuhl, J.-C. Leyer, A. A. Borisov and W. A. Sirignano, *Progress in Astronautics and Aeronautics Series*, **152**, AIAA, New York (1991), pp. 365-382.

[59] Oppenheim, A. K. and Maxson, J. A., "A Thermochemical Phase Space for Combustion in Engines", *Twenty-Fifth Symposium (Int.) on Combustion*, Combustion Institute, Pittsburgh, PA (1994), pp. 157-165.

[60] Kuhl, A. L., Ferguson, R. E., and Oppenheim, A. K., "Gasdynamic Model of Turbulent Exothermic Fields in Explosions", *Advances in Combustion Science—in Honor of Ya. B. Zel'dovich*, edited by A. N. Merzhanov, L. DeLuca and W. A. Sirignano, *Progress in Astronautics and Aeronautics Series*, **173**, AIAA, Washington, DC (1997), pp. 251-261.

[61] Kuhl, A. L., Ferguson, R. E., Reichenbach, H., Neuwald, P., and Oppenheim, A.K., "Dynamics of an Explosion-Driven Planar Exothermic Jet", *JSME Int. Journal—Series B*, **41** (2), (1998), pp. 416-423.

[62] Cybulski,W.,: "Detonation of Coal Dust", *Bulletin de L'Academie Polonaise des Sciences*, **19**, 1971, pp.37-41.

[63] Cybulski, W., *Wybuchy pylu weglowego i ich zwalczanie*, Slosk, 1973, 451 pp.; *Coal Dust Explosions and Their Suppression*, translated by Z. Zienkiewicz, Warsaw, Poland, published by U. S. Bureau of Mines, Washington, DC, 1975, 583 pp. {NTIS number TT 73-54001}.

[64] Kuhl, A. L., "Spherical Mixing Layers in Explosions", *Dynamics of Exothermicity*, J.R. Bowen Editor, Gordon and Breach Publishers, Longhorn, PA (1996), pp. 291-320.

[65] Kuhl, A. L., and Oppenheim, A.K.,"Turbulent Combustion in the Self-Similar Exothermic-Flow Limit", *Advanced Computation and Analysis of Combustion*, Edited by G. D. Roy, S. M. Frolov and P. Givi, ENAS Publishers, Moscow, 1997, pp. 388-396.

[66] Colella, P. and Glaz, H. M., "Efficient Solution Algorithms for the Riemann Problem fro Real Gases", *J. Computational Physics*, **59** (2), 1985, pp. 264-289.

[67] Berger, M. J. and Colella, P., "Local Adaptive Mesh Refinement for Shock Hydrodynamics", *J. Computational Physics*, **82** (1), 1989, pp. 64-84.

[68] Bell, J. B., Berger, M., Saltzman, J., Welcome, M., "Three-Dimensional Adaptive Mesh Refinement for Hyperbolic Conservation Laws," *SIAM Journal on Scientific and Statistical Computing*, **15** (1), 1994, pp. 127-138.

[69] Bell, J. B., and Marcus, D. L., "Vorticity Intensification and Transition to Turbulence in the 3-D Euler Equations", *Comm. Math. Phys.*, **147**, 1992, pp. 374-394.

[70] Dobratz, B., "Properties of Chemical Explsives and Explosive Simulants", Lawrence Livermore National Laboratory, UCRL-**51319**, Livermore, CA, 1974.

[71] Taylor, G. I., "The Dynamics of the Combustion Products Behind Plane and Spherical Detonation Fronts in Explosives", *Proc. Royal Soc.*, Series A, **200**, 1950, pp. 235-247.

[72] Sedov, L.I., *Similarity and Dimensional Methods in Mechanics*, M. Friedman translator, M. Holt editor, Academic Press, 1959, (vid. esp. Chapter IV).

[73] Reynolds, W.C., *'STANJAN" Interactive Computer Programs for Chemical Equilibrium Analysis*, Department of Mechanical Engineering, Stanford University, Stanford ,California, 1986, 48 pp.
(74) Shvab, V. A., "Sviaz Miezdy Temperaturnymi i Skorostnymi Polyami Gazovogo Fakiela" ("Relationship between Temperature and Velocity Fields in Gaseous Flames"), *Zh. Tech. Fiz.*, **11** (5), 1941, pp. 431-442.

(75) Zel'dovich, Ya. B., "K Teorii Goreniya Ne Peremeshannykh Gazov" ("On the Theory of Combustion of Initially Unmixed Gases") *Zh. Tekh. Fiz.*, **19** (10), 1949, pp. 1199-1210.

[76] Richtmyer, R. D., "Taylor Instability in Shock Acceleration of Compressible Fluids", *Comm. Pure Appl. Math*, **13**, 1960, pp. 297-319.

[77] Meshkov, E. E., "Instability of the Interface of Two Gases Accelerated by a Shock Wave", *Izv AN SSRE Mekhanika Zhidkosti i Gaza*, **4** (15), 1960, pp. 151-157.

[78] Anisimov, S. I., and Zel'dovich, Ya. B., "Rayleigh-Taylor Instability of Boundary between Detonation Products and Gas in Spherical Explosion", *Pis'ma Zh. Eksp. Teor. Fiz.*, **3**, 1977, pp. 1081-1084.

[79] Anisimov, S. I., Zel'dovich, Ya. B., Inogamov, M. A. and Ivanov, M. F., "The Taylor Instability of Contact Boundary between Expanding Detonation Products and a Surrounding Gas", *Shock Waves, Explosions and Detonations*, J. R. Bowen, J.-C. Leyer, and R. I. Soloukhin, Eds., Progress in Astronautics and Aeronautics Series (M. Summerfield, Editor-in-Chief), **87**, AIAA, Washington, D.C., 1983, pp. 218-227.

[80] Peters, N., "Length Scales in Laminar and Turbulent Flames", *Numerical Approaches to Combustion Modeling*, E. S. Oran and J. P. Boris Editors, Progress in Astronautics and Aeronautics (A. R. Seebass Editor-in-Chief), **135**, AIAA, Washington DC., 1991, pp. 155-182.

[81] Liñán, A., and Williams, F. A., *Fundamental Aspects of Combustion*, Oxford University Press, New York and Oxford (vid. esp. Chapter 5 : Turbulent Combustion, pp. 132-140), 1993.